

# Uniform approximation for diffractive contributions to the trace formula in billiard systems

Martin Sieber<sup>1,2</sup>, Nicolas Pavloff<sup>1</sup> and Charles Schmit<sup>1</sup>

<sup>1</sup> Division de Physique Théorique\*, Institut de Physique Nucléaire, F-91406 Orsay Cedex, France

<sup>2</sup> Institut für Theoretische Physik, Universität Ulm, D-89069 Ulm, Germany

## Abstract

We derive contributions to the trace formula for the spectral density accounting for the role of diffractive orbits in two-dimensional billiard systems with corners. This is achieved by using the exact Sommerfeld solution for the Green function of a wedge. We obtain a uniformly valid formula which interpolates between formerly separate approaches (the geometrical theory of diffraction and Gutzwiller's trace formula). It yields excellent numerical agreement with exact quantum results, also in cases where other methods fail.

PACS numbers:

03.40.Kf Waves and wave propagation: general mathematical aspects.

03.65.Sq Semiclassical theories and applications.

05.45.+b Theory and models of chaotic systems.

IPNO/TH 96-22 ULM-TP/96-3 *submitted to Physical Review E*

---

\*Unité de Recherche des Universités Paris XI et Paris VI associée au CNRS

# 1 Introduction

Two-dimensional classical billiards became popular as model systems exhibiting a rich variety of dynamical behaviour, ranging from integrable to fully chaotic. Their quantum counterparts attracted much interest starting in the 80's, both from the point of view of random matrix theory and the semiclassical periodic orbit theory. In the latter approach one uses trace formulae of the type first derived by Gutzwiller [1] and Balian and Bloch [2, 3].

During the last two years, following the route opened by Ref. [4], a number of studies (see Refs. [5, 6, 7, 8]) have concentrated on additional contributions to the trace formula linked to diffractive effects near regions where the classical Hamiltonian flow is discontinuous. These zones of discontinuity are known as “optical boundaries” in the literature. They lead to contributions from non-classical (so-called diffractive) orbits hitting a corner of the billiard or creeping around a smooth boundary.

Apart from the noticeable exception of Ref. [7] all the work quoted above is based on Keller's “geometrical theory of diffraction” (GTD, see e.g. [9]), i.e. on an extension of geometrical optics which accounts for diffractive effects. Keller's approach fails when the diffractive trajectory is very close to an optical boundary, or equivalently when the diffractive orbit is close to become an allowed classical trajectory (this will be clarified in the text of the paper). In the present work we use a uniform approximation for the Green function which does not have this drawback. This allows to derive relatively simple formulae which are uniformly valid. The method is applied to billiards whose boundary has a slope discontinuity and thus we restrict our study to wedge diffraction effects. To our knowledge there does not yet exist a uniformly valid formula for the contributions of creeping orbits (despite the progress made in Ref. [7]).

The theory of uniform approximations for wedge diffraction has a long history which begins with a famous paper by Pauli [10]. In the late 60's and in the 70's the problem has been studied in detail. Much literature has been devoted to several types of approaches remedying the deficiency of the geometrical theory of diffraction. The approach most widely used is known as “uniform asymptotic theory” and was developed by Ahluwalia, Boersma, Lewis and coworkers in Refs. [11, 12, 13, 14]. We have chosen here a technique more closely related to the original work of Sommerfeld and Pauli. It relies on an extension of the method of steepest descent due to Pauli which was carefully studied on a general setting by Clemmow [15]. The method, due to Kouyoumjian and Pathak, is known as “uniform theory of diffraction” and is exposed in Refs. [16] and [17]. Note that we apply the uniform approximation only to orbits with a single diffractive point. The treatment of multiple wedge diffraction is increasingly more involved as can be seen in work on double diffraction by half-planes (see Refs. [18, 19, 20]) or wedges [21]. To our knowledge there does not exist to date a general uniform approximation for multiple wedge diffraction.

The paper is organized as follows. In the next section we recall the exact solution of the infinite wedge problem, derive a uniform approximation for the Green function and compare it with the result obtained from GTD. In Sec. 3 we use the Green function obtained previously to derive contributions to the trace formula which are uniformly valid. Readers mostly interested in the final result can skip this part and go directly to Sec. 4, where we discuss the previously obtained formula and several of its limits. In particular, we show that this formula has the appealing feature of interpolating between the semiclassical results of periodic orbit theory and the formulae obtained in Refs. [4, 6, 8]. Sec. 5 contains numerical applications for several simple billiard systems. In some cases GTD gives reasonable results, but in other cases the uniform approximation has to be used in order to describe the Fourier transform

of the spectral density correctly. Finally we discuss our results and possible extensions in Sec. 6.

## 2 The Green function of an infinite wedge

In this section we consider an infinite wedge of interior angle  $\gamma$  ( $\gamma \in ]0, 2\pi[$ ) with Dirichlet boundary conditions and derive several approximations for the Green function.

### 2.1 The exact result

The exact solution of the problem was first given by Sommerfeld for a wedge with  $\gamma = 2\pi$  (a half line) and an incident plane wave, see [22]. The solution of the general problem is easily inferred from his approach, a complete treatment is given for instance by Carslaw in Refs. [23, 24]. We recall here for completeness some properties of the solution.

The Green function  $G_\gamma(\vec{r}, \vec{r}', E)$  of the problem in dimensionless units is a solution of:

$$\begin{aligned} (\Delta_{\vec{r}} + E)G_\gamma(\vec{r}, \vec{r}', E) &= \delta(\vec{r} - \vec{r}'), \\ G_\gamma &\equiv 0 \quad \text{if } \vec{r} \text{ or } \vec{r}' \text{ are on the boundary.} \end{aligned} \quad (1)$$

Choosing a system of coordinates with the origin at the vertex and the polar axis along one of the boundaries such that  $\theta$  and  $\theta'$  are in  $[0, \gamma]$  (see Fig. (2a)), one can write the following integral representation for the exact solution:

$$G_\gamma(\vec{r}, \vec{r}', E) = g_\gamma(r, r', \theta' - \theta) - g_\gamma(r, r', \theta' + \theta), \quad (2)$$

with

$$g_\gamma(r, r', \phi_\sigma) = -\frac{i}{8\pi N} \int_{A+B} dz \frac{H_0^{(1)}\left(k\sqrt{r^2 + r'^2 - 2rr'\cos z}\right)}{1 - \exp\left[-i\frac{z - \phi_\sigma}{N}\right]}. \quad (3)$$

In (3) and in the following the angles  $\theta$  and  $\theta'$  always appear in the combination  $\theta' \pm \theta$  and we will denote  $\phi_\sigma = \theta' - \sigma\theta$  ( $\sigma = \pm 1$ ). Other quantities appearing in (3) are  $N = \gamma/\pi$ ,  $k = \sqrt{E}$  which is the modulus of the wave-vector,  $H_0^{(1)}$  which is the Hankel function of the first kind (see [25]), and  $A$  and  $B$  which are the contours in the complex plane drawn in Fig. 1. In this figure one can further see the poles of the integrand corresponding to  $(z - \phi_\sigma)/N = 2n\pi$  (with  $n \in \mathbb{Z}$ ) – they appear as black points – and branch cuts linked to the square root argument of  $H_0^{(1)}$ . The shaded areas are zones where the integrand increases without limit when one goes away from the real axis (this is easily checked by using the leading asymptotic term (7) of the Hankel function). The integration contour is quite arbitrary as long as it goes to infinity in the indicated unshaded regions.

Essentially,  $g_\gamma$  is a superposition of free Green functions (with complex angles  $z$ ). Considered as a function of  $\phi_\sigma$ , it has periodicity  $2\pi N = 2\gamma$  and this ensures that the Green function (2) satisfies the boundary conditions for  $\theta = 0$  and  $\gamma$ . By moving the contours  $A$  and  $B$  towards the real line  $z \in [-\pi, \pi]$  and taking into account the poles of the integrand one obtains

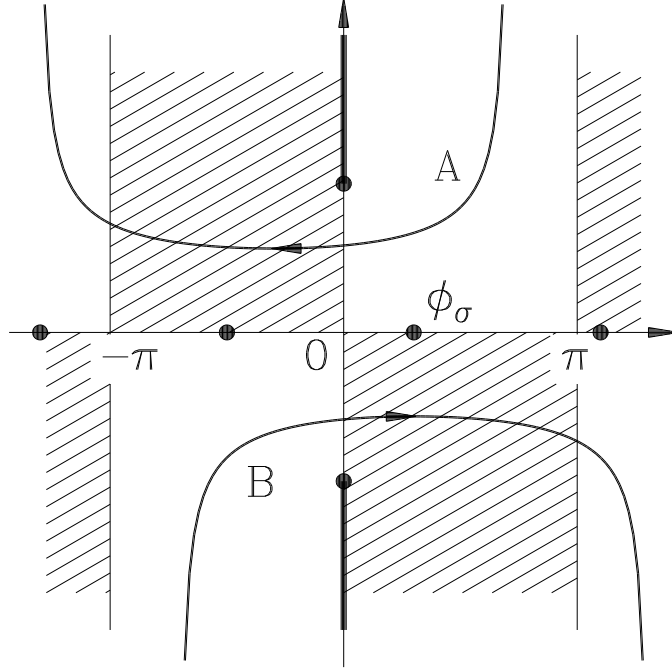


Figure 1: Integration contour in the complex plane for formula (3). The shaded areas are zones where the integrand diverges when going away from the real axis. The black points are poles and branch points of the integrand. The thick lines are branch cuts.

$$g_\gamma(r, r', \phi_\sigma) = -\frac{i}{4} \sum'_n H_0^{(1)} \left( k \sqrt{r^2 + r'^2 - 2rr' \cos(\phi_\sigma - 2n\gamma)} \right) + h_\gamma(r, r', \phi_\sigma), \quad (4)$$

where after a change of variable  $h_\gamma$  can be written in the form

$$h_\gamma(r, r', \phi_\sigma) = \frac{\sin(\pi/N)}{8\pi N} \int_{-i\infty}^{+i\infty} dz \frac{H_0^{(1)} \left( k \sqrt{r^2 + r'^2 + 2rr' \cos z} \right)}{\cos\left(\frac{z + \phi_\sigma}{N}\right) - \cos(\pi/N)}. \quad (5)$$

The first term on the r.h.s. of (4) contains the contributions of those poles of the integrand of (3) which lie between  $-\pi$  and  $\pi$ ; the prime indicates that the summation is restricted to values of  $n$  such that  $-\pi \leq \phi_\sigma - 2n\gamma \leq \pi$ . If  $\phi_\sigma$  is exactly equal to  $\pm\pi + 2n\gamma$  then the corresponding contribution to the summation has to be divided by 2. In (5) the contour can be modified as long as no pole of the integrand is crossed. A further requirement is that the part of the contour extending to infinity has to start at  $-i\infty$  with a real part in  $[0, \pi[$  and to extend to  $i\infty$  with a real part in  $] -\pi, 0]$ .

The discrete summation in (4) can be interpreted as arising from allowed classical trajectories. For instance the case  $\phi_+ = \theta' - \theta$  and  $n = 0$  gives a contribution  $-(i/4)H_0^{(1)}(k|\vec{r}' - \vec{r}|)$  and corresponds to the free propagation from  $\vec{r}'$  to  $\vec{r}$ . The other terms in the summation correspond to trajectories

experiencing specular reflections on the boundaries (this is illustrated in Fig. (2b)). If  $\sigma = 1$  (resp.  $\sigma = -1$ ) the orbit has an even (resp. odd) number of reflections. These orbits correspond to successive applications of the method of images and their contribution is known as the geometrical term in the literature. When inserted back in Eq. (2) they give a term which will be denoted  $G_{geo}(\vec{r}, \vec{r}', E)$  in the following.

If the angle  $\gamma$  is of the form  $\pi/p$  ( $p \in \mathbb{N}^*$ ) then  $\sin(\pi/N) = 0$  and the term  $h_\gamma(r, r', \phi_\sigma)$  is zero: the geometrical term alone is enough to fulfill the boundary conditions. This is due to the fact that in this case the Green function can be determined by the method of images. If  $\gamma \neq \pi/p$ , then  $h_\gamma$  corresponds to the contribution from diffraction. Hence the total Green function can be written as a sum of a geometrical plus a diffractive term:

$$\begin{aligned} G_\gamma(\vec{r}, \vec{r}', E) &= G_{geo}(\vec{r}, \vec{r}', E) + G_{diff}(\vec{r}, \vec{r}', E), \\ \text{with } G_{diff}(\vec{r}, \vec{r}', E) &= h_\gamma(r, r', \theta' - \theta) - h_\gamma(r, r', \theta' + \theta). \end{aligned} \quad (6)$$

## 2.2 Geometrical theory of diffraction

We derive now a simple approximation for  $G_{diff}$ . We first replace the Hankel function by its asymptotic form for large arguments (see [25]):

$$H_0^{(1)}(z) \approx \sqrt{\frac{2}{\pi z}} e^{iz - i\pi/4} \quad \text{when } |z| \gg 1. \quad (7)$$

The same approximation is used also in all the following for the geometrical and diffractive Green functions, i.e. for all the terms of Eqs. (4) and (5), the assumption being that the distances measured along the paths (classical or diffractive) going from  $\vec{r}'$  to  $\vec{r}$  are large compared to the wavelength  $\lambda = 2\pi/k$ . Then in the integral defining  $h_\gamma$  there is a saddle point of the exponent at  $z = 0$  and a steepest descent approximation yields:

$$h_\gamma(r, r', \phi_\sigma) \approx \frac{1}{4\pi N} \frac{\sin(\pi/N)}{\cos(\phi_\sigma/N) - \cos(\pi/N)} \frac{e^{ik(r+r') + i\pi/2}}{k\sqrt{rr'}}. \quad (8)$$

Incorporating this result into the expression (6) for  $G_{diff}$  one obtains a formula which can be cast into the form:

$$G_{diff}(\vec{r}, \vec{r}', E) \approx G_{sc}(\vec{r}, \vec{r}_0, E) \mathcal{D}(\theta, \theta') G_{sc}(\vec{r}_0, \vec{r}', E), \quad (9)$$

with

$$\begin{aligned} \mathcal{D}(\theta, \theta') &= \frac{2}{N} \sin \frac{\pi}{N} \left[ \left( \cos \frac{\pi}{N} - \cos \frac{\theta + \theta'}{N} \right)^{-1} - \left( \cos \frac{\pi}{N} - \cos \frac{\theta - \theta'}{N} \right)^{-1} \right] \\ &= -\frac{4}{N} \frac{\sin(\pi/N) \sin(\theta/N) \sin(\theta'/N)}{\left( \cos \frac{\pi}{N} - \cos \frac{\theta + \theta'}{N} \right) \left( \cos \frac{\pi}{N} - \cos \frac{\theta - \theta'}{N} \right)}. \end{aligned} \quad (10)$$

In (9)  $G_{sc}$  is the free Green function evaluated using (7) and  $\vec{r}_0$  is the point at the vertex (see Fig. (2a)). Expressions (9) and (10) give the diffractive part of the Green function in the “geometrical theory of diffraction” (see [9]). They have the simple interpretation as being the contribution of a (non-classical) diffractive trajectory going from  $\vec{r}'$  to  $\vec{r}_0$  and then from  $\vec{r}_0$  to  $\vec{r}$  (see Fig. (2b)). Using this approximation one can derive a trace formula for the spectral density which accounts for diffractive effects in the GTD approximation (see Refs. [4, 6, 8]).

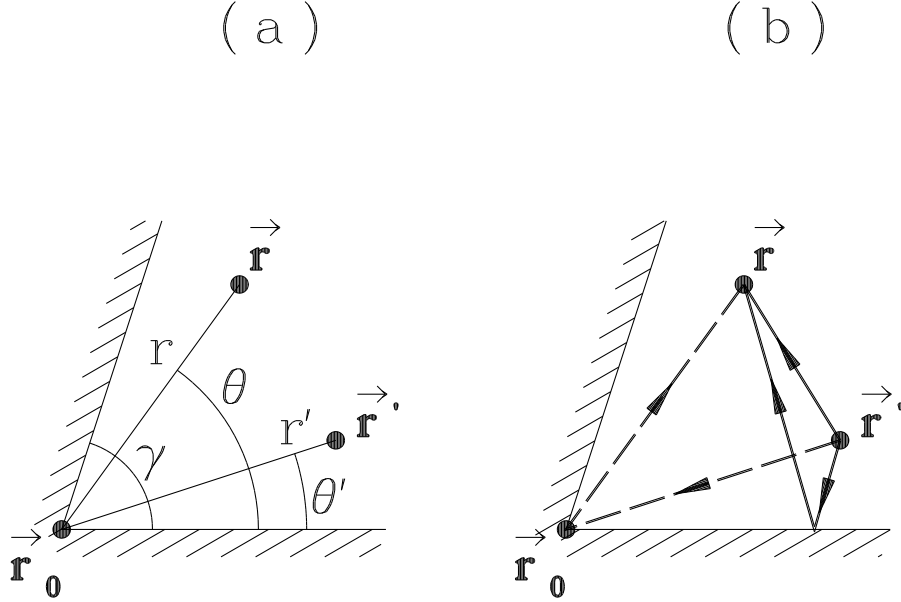


Figure 2: Figure (a) displays the notations used in the text. Figure (b) shows two classical trajectories (solid lines) and the diffractive orbit going from  $\vec{r}'$  to  $\vec{r}$  (dashed line).

The quantity  $\mathcal{D}(\theta, \theta')$  is known as the diffraction coefficient. It is zero if  $\theta$  (or  $\theta'$ ) is equal to 0 or  $\gamma$ , or if  $\pi/\gamma$  is an integer. It diverges on an optical boundary, i. e. if  $\vec{r}$  and  $\vec{r}'$  are such that the diffractive orbit is the limit of a classical trajectory. This is illustrated by the simple case of diffraction by a sharp wedge ( $\gamma > 3\pi/2$ ) in Fig. 3. In this case there are two optical boundaries represented by dashed lines. They correspond to  $\theta = \theta' + \pi$  (i. e.  $\phi_+ = \theta' - \theta = -\pi$ ) and  $\theta = \pi - \theta'$  (i. e.  $\phi_- = \theta' + \theta = \pi$ ). In the terminology of geometrical optics, the first optical boundary separates the illuminated and shadowed regions for direct rays when the point  $\vec{r}'$  is considered as a light source (boundary between regions II and III), and the second optical boundary separates the illuminated and shadowed regions for rays that are reflected on one side of the wedge (boundary between regions I and II). If  $\vec{r}$  lies near one of the optical boundaries then the diffractive path is almost an allowed classical trajectory, and if  $\vec{r}$  is moved onto an optical boundary then the diffractive path coincides in this limit with an allowed classical trajectory.

Looking in more detail at the origin of the divergence, one sees from Eq. (8) that it occurs when there exists an integer  $n$  such that  $\phi_\sigma = \pm\pi + 2nN\pi$ . In this case there is a pole  $z = \phi_\sigma \mp \pi - 2nN\pi = 0$  in the integral representation of the diffractive part (5) which is at the same position as the saddle

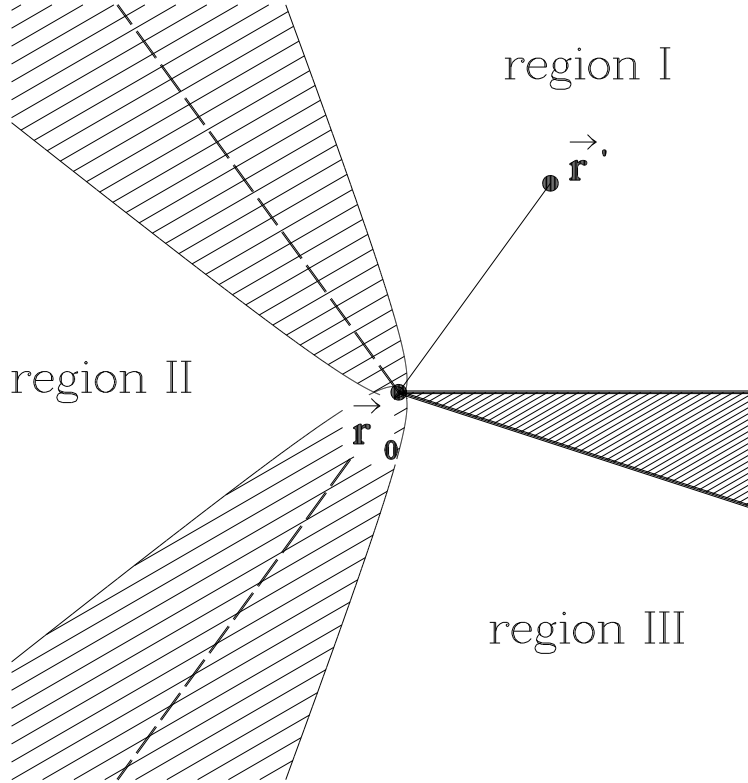


Figure 3: Optical boundaries (dashed lines) for an initial point  $\vec{r}'$  in the case of diffraction by a sharp wedge ( $\gamma > 3\pi/2$ ). The transition regions (for  $r' = 10\lambda$ ) around the optical boundaries are shaded.

point  $z = 0$  and thus the saddle point approximation breaks down. More generally, the geometrical theory of diffraction is only valid if all poles are sufficiently far away from the saddle point  $z = 0$ . This can be interpreted in terms of the physical trajectories in the system because, in Sommerfeld's solution (2,3), the saddle point corresponds to the diffractive orbit and the poles correspond to geometrical orbits.

### 2.3 A uniform approximation

As seen above, one has to refine the steepest descent evaluation of  $h_\gamma$  in case that there is a pole of the integrand near the saddle point  $z = 0$ . This was first done by Pauli [10] and we present here a slight modification of the original procedure [16, 17]. In a first step one can separate poles which are possibly near one another by using the identity:

$$\frac{2 \sin(\pi/N)}{\cos\left(\frac{z + \phi_\sigma}{N}\right) - \cos(\pi/N)} = \frac{1}{\tan\left(\frac{z + \phi_\sigma + \pi}{2N}\right)} - \frac{1}{\tan\left(\frac{z + \phi_\sigma - \pi}{2N}\right)}. \quad (11)$$

Hence  $h_\gamma$  in Eq. (5) can be rewritten as

$$h_\gamma(r', r, \phi_\sigma) = u_{\gamma,+}(r', r, \phi_\sigma) - u_{\gamma,-}(r', r, \phi_\sigma), \quad (12)$$

where

$$u_{\gamma,\eta}(r, r', \phi_\sigma) = \frac{1}{16\pi N} \int_{-i\infty}^{+i\infty} dz \frac{H_0^{(1)}\left(k\sqrt{r^2 + r'^2 + 2rr' \cos z}\right)}{\tan\left(\frac{z + \phi_\sigma + \eta\pi}{2N}\right)}, \quad (13)$$

and  $\eta = \pm 1$  is a new index.

If one denotes by  $n_{\sigma,\eta}$  the nearest integer to  $(\phi_\sigma + \eta\pi)/(2\gamma)$  then  $z = -(\phi_\sigma + \eta\pi) + 2n_{\sigma,\eta}\gamma$  is the pole of the integrand of (13) which is nearest to the saddle point  $z = 0$ . Thanks to the separation (12) the next pole in the integrand of (13) is at distance  $2\gamma$  and its effect can safely be neglected if  $\gamma$  is not a small angle (this will be assumed in the following). According to the method of Pauli one rewrites the integrand by multiplying numerator and denominator by a function imitating the behaviour of the original denominator but in which the  $z$  and  $\phi_\sigma$  parts are separated. This procedure is not unique, it corresponds to a specific choice of a uniform approximation as will be discussed below. The choice for the function is  $\eta\sqrt{2}\sin(z/2) + a_{\sigma,\eta}$ , where  $a_{\sigma,\eta}$  is a measure of the separation between the saddle point  $z = 0$  and the nearest optical boundary:

$$a_{\sigma,\eta} = \sqrt{2} \cos\left(\frac{\phi_\sigma}{2} - n_{\sigma,\eta}\gamma\right) \quad \text{with} \quad n_{\sigma,\eta} = \text{nint}\left[\frac{\phi_\sigma + \eta\pi}{2\gamma}\right] \in \mathbb{Z}. \quad (14)$$

Using the asymptotic formula (7) for the Hankel function one obtains:

$$u_{\gamma,\eta}(r, r', \phi_\sigma) \approx \frac{e^{-i\pi/4}}{8\gamma\sqrt{2\pi k}} \int_{-i\infty}^{+i\infty} dz \frac{e^{ik\sqrt{r^2 + r'^2 + 2rr' \cos z}}}{\eta\sqrt{2}\sin(z/2) + a_{\sigma,\eta}} F^{\sigma,\eta}(z), \quad (15)$$

where  $F^{\sigma,\eta}(z)$  is a smooth function at  $z = 0$ , even in the vicinity of an optical boundary (when  $a_{\sigma,\eta} \rightarrow 0$ , see (20)):

$$F^{\sigma,\eta}(z) = \frac{\eta\sqrt{2}\sin(z/2) + a_{\sigma,\eta}}{(r^2 + r'^2 + 2rr' \cos z)^{1/4} \tan\left(\frac{z + \phi_\sigma + \eta\pi}{2N}\right)}.$$

Note that the integrands of (15) and (13) both have the pole  $z = -(\phi_\sigma + \eta\pi) + 2n_{\sigma,\eta}\gamma$  next to the origin as mentioned above.

Now (15) is evaluated along the steepest descent path at  $z = 0$  by a change of variable  $z = \eta t\sqrt{2}\exp(i3\pi/4)$  with  $t \in \mathbb{R}$  (the factor  $\eta\sqrt{2}$  is here for convenience). The smooth, non-singular part  $F^{\sigma,\eta}$  of the integrand is simply evaluated at  $t = 0$ , and the phase of the exponential function and the denominator are expanded in the vicinity of the origin:

$$\eta\sqrt{2}\sin(z/2) + a_{\sigma,\eta} = a_{\sigma,\eta} + t e^{3i\pi/4} + \mathcal{O}(t^3), \quad (16)$$

and



$$ik\sqrt{r^2 + r'^2 + 2rr' \cos z} = ik(r + r') - \frac{kr r'}{r + r'} t^2 + \mathcal{O}(t^3). \quad (17)$$

Hence  $u_{\gamma,\eta}$  is approximated by:

$$u_{\gamma,\eta}(r, r', \phi_\sigma) \approx \frac{e^{ik(r + r') - i\pi/4}}{8\gamma\sqrt{\pi k(r + r')}} \frac{a_{\sigma,\eta}}{\tan\left(\frac{\phi_\sigma + \eta\pi}{2N}\right)} \int_{-\infty}^{\infty} dt \frac{\exp\left[-krr't^2/(r + r')\right]}{t - a_{\sigma,\eta}e^{i\pi/4}}. \quad (18)$$

After the expansion (16) of the denominator, the pole in (18) is only approximately equal to the nearest pole in (13), but they coincide when the pole approaches the stationary point  $t = 0$ . As noted above the choice of the uniform approximation which leads to Eq. (18) is not unique (as discussed by Clemmow, who calls it a “partial asymptotic expansion”, see [15]). For example, another choice of a uniform approximation can be obtained by making a change of variable which transforms the exponent in (15) such that it becomes an exact quadratic function, and multiply denominator and integrand by a function which is linear in the new variable. Then one obtains Eq. (18) with a different definition of  $a_{\sigma,\eta}$  which is expressed in terms of a “detour parameter” such as used in the “uniform approximation theory” (see Refs. [11, 12, 13, 14]). In practical applications, however, the differences between different uniform approximations are small. We would like to add that the uniform approximations can be further improved by including also sub-leading terms of the asymptotic expansion of the Hankel function and also higher order terms of the expansion of the integrand (see Refs. [10, 15]). However, numerical checks show (see Fig. 4 and below) that such refinements are not necessary here.

We continue now with the integral (18) which can be recognized as an integral representation of the modified Fresnel function  $K$  (see Appendix A and Eq. (A5)) and the final expression for the uniform approximation for  $u_{\gamma,\eta}$  is:

$$u_{\gamma,\eta}(r, r', \phi_\sigma) \approx \frac{1}{4N} \frac{e^{ik(r + r') + i\pi/4}}{\sqrt{\pi k(r + r')}} \frac{|a_{\sigma,\eta}|}{\tan\left(\frac{\phi_\sigma + \eta\pi}{2N}\right)} K\left(|a_{\sigma,\eta}| \sqrt{\frac{kr r'}{r + r'}}\right). \quad (19)$$

This expression remains finite on the optical boundary  $\phi_\sigma = -\eta\pi + 2n_{\sigma,\eta}\gamma$ . As an optical boundary is crossed,  $a_{\sigma,\eta}$  goes through zero and changes sign and one has:

$$\frac{|a_{\sigma,\eta}|}{\tan\left(\frac{\phi_\sigma + \eta\pi}{2N}\right)} \approx \eta\sqrt{2N} \operatorname{sign}(a_{\sigma,\eta}) \quad \text{when} \quad a_{\sigma,\eta} \rightarrow 0. \quad (20)$$

Hence although the problem of divergence has been eliminated one arrives at a final form which is discontinuous. This was expected: the exact terms (5) and (13) already have this behaviour; because of the separation (6) of the total Green function into a geometrical and a diffractive term, each contribution ( $G_{geo}$  and  $G_{diff}$ ) is discontinuous at the optical boundary, but their sum is continuous.

As a résumé of the results of this section we write down the uniform approximation for the diffractive part of the Green function which is a sum of four contributions:

$$G_{diff}(\vec{r}, \vec{r}', E) \approx \frac{1}{4N} \frac{e^{ik(r+r') + i\pi/4}}{\sqrt{\pi k(r+r')}} \sum_{\sigma, \eta = \pm 1} \frac{\sigma \eta |a_{\sigma, \eta}|}{\tan\left(\frac{\phi_{\sigma} + \eta \pi}{2N}\right)} K\left(|a_{\sigma, \eta}| \sqrt{\frac{kr r'}{r+r'}}\right), \quad (21)$$

where  $\phi_{\sigma} = \theta' - \sigma \theta$  ( $\theta$  and  $\theta'$  being chosen in  $[0, \gamma]$ ) and  $a_{\sigma, \eta}$  is defined in (14).

In the remaining part of this section we present some numerical results illustrating the accuracy of the uniform approximation and a failure of the GTD approximation. If the next optical boundary is sufficiently far away one can replace the modified Fresnel function in (21) by the first term of its asymptotic expansion (A4) and this leads to the GTD result (9,10). Roughly speaking, this approximation is good when the argument of the  $K$ -function is greater than 3 and it fails when the argument is less than 1.5. This puts a limit on the use of the geometrical theory of diffraction illustrated in Fig. 3: inside the dashed areas around the optical boundaries one has to use the uniform approximation (these zones are known as “transition region” in the literature). The figure has been drawn for the case  $r' = 10\lambda$  ( $\lambda = 2\pi/k$ ), and the transition regions are larger if one goes to smaller values of  $r'/\lambda$ . In the limit  $r \gg r' \gg \lambda$ , the transition width around an optical boundary at distance  $r$  from the apex is proportional to  $r\sqrt{\lambda/r'}$  (relying on the weaker assumption that  $r, r' \gg \lambda$  one can show that it is proportional to  $[\lambda(r^2 + rr')/r']^{1/2}$ ). Outside of the transition region expression (9,10) is valid and shows that  $G_{diff}$  is a small correction to  $G_{geo}$ . But near the optical boundary the two terms are of the same order and exactly on the boundary the two discontinuous contributions to  $G_{geo}$  and  $G_{diff}$  have exactly the same amplitude.

The comparison between the uniform approximation (21), the geometrical theory of diffraction (9,10) and the exact result (5,6) for  $G_{diff}$  is made quantitative in Fig. 4. In this figure one considers a wedge of interior angle  $\gamma = 110^\circ$ . The source point  $\vec{r}'$  is fixed at  $\theta' = 60^\circ$  and  $r' = 5\lambda$ . The observation point  $\vec{r}$  is at fixed distance from the vertex ( $r = r'$ ) and  $\theta$  scans the interval  $[0, \gamma]$ . The modulus of  $G_{diff}$  is then plotted as a function of  $\theta$ . In the figure one cannot distinguish the uniform approximation from the exact result. The geometrical theory of diffraction diverges on the optical boundaries (represented as dashed lines in the upper part of Fig. 4). Furthermore it is in clear disagreement with the exact result for all values of  $\theta$ . Hence one can infer that a trace formula based on Eq. (9) will not correctly describe the spectrum in cases such as presented in Figure 4.

### 3 Diffractive orbits in the trace formula

We consider now a closed two-dimensional region  $\mathcal{B}$  with a boundary  $\partial\mathcal{B}$  smooth everywhere except at a finite number of points where its slope is discontinuous. The spectral density  $d(k)$  of this system has semiclassical contributions from periodic orbits as well as from diffractive orbits. The latter ones are closed orbits which have a finite number of points on vertices of the billiard (we call these points diffractive or corner points in the following) and follow the law of geometrical optics between two diffractive points. Within the framework of the geometrical theory of diffraction, the contribution of a diffractive orbit  $\xi$  to the level density has been derived in [4, 6, 8] and it is given by

$$d_{\xi}(k) = \frac{L_0}{\pi} \left[ \prod_{i=1}^p \frac{\mathcal{D}_i}{\sqrt{8\pi k (M_i)_{12}}} \right] \cos\left(kL - \frac{\pi}{2}\nu - \frac{3\pi}{4}p\right). \quad (22)$$

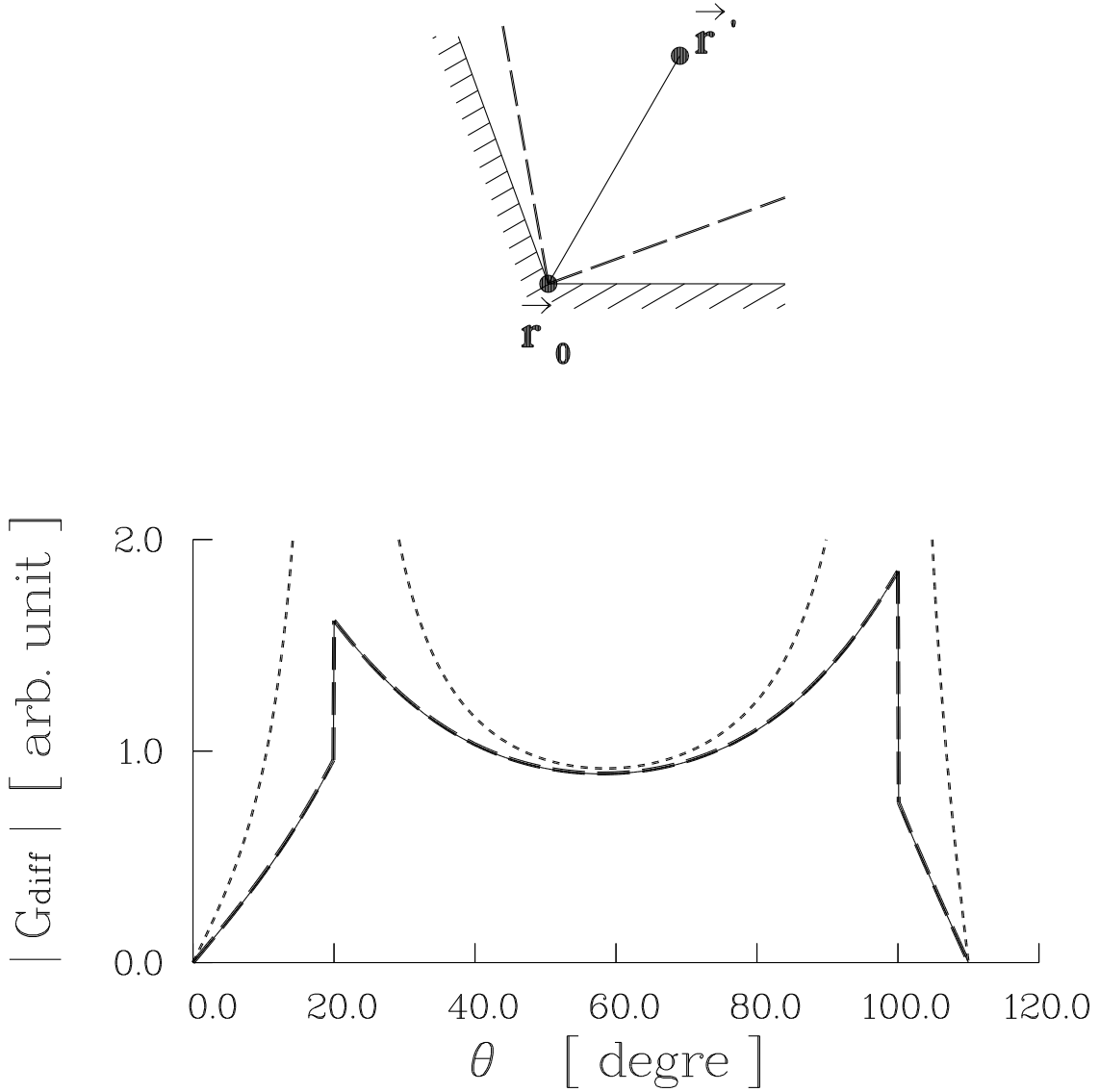


Figure 4: Modulus of  $G_{diff}(\vec{r}, \vec{r}', E)$  for fixed  $\vec{r}'$  and  $r$  in a wedge with  $\gamma = 110^\circ$  ( $r = r' = 5\lambda$  and  $\theta' = 60^\circ$ ).  $\theta$  scans the interval  $[0, \gamma]$ . The upper part of the figure displays the geometry considered, the optical boundaries appearing as dashed lines. In the lower part, the solid line is the exact result (5,6), the long dashed line is the uniform approximation (21) and the short dashed line is the GTD result (9,10).

Here  $L_0$  and  $L$  are the primitive and total length of the trajectory, respectively,  $p$  is the number of diffractive points,  $\mathcal{D}_i$  is the diffraction coefficient in the  $i$ -th corner (cf. Eq. (10)),  $(M_i)_{12}$  is the (12)-element of the stability matrix at unit energy for a part of the trajectory between two corners, and  $\nu$  is the number of conjugate points plus twice the number of reflections on the boundary between corners.

According to (22) each corner point decreases the contribution of a diffractive orbit by an order  $\mathcal{O}(k^{-1/2})$ . This is correct only if the diffractive trajectory is sufficiently far away from the optical boundaries in every corner point. In the opposite case that the trajectory lies on an optical boundary in every corner point it can be shown that its contribution is of the same order in  $k$  as that of a regular periodic orbit (see below). In the following we will go beyond the GTD approximation and derive a contribution to  $d(k)$  from diffractive orbits with one point in a corner that interpolates between these two regimes. We will use for this purpose a method of uniform approximation similar to that exposed in the previous section.

The starting point of our derivation is the boundary element method. It is a reformulation of the quantum mechanical eigenvalue problem in terms of a Fredholm equation of the second kind for the normal derivative of the wave function on the boundary (see e. g. Refs. [26, 27, 28, 29, 30] for discussion and application in the context of the trace formula). More specifically if we denote by  $\vec{r}(s)$  a point of the boundary with curvilinear abscissa  $s$  and by  $u(s)$  the normal derivative of the wave function at this point, one has the following integral equation for the case of Dirichlet boundary conditions:

$$u(s') = -2 \int_{\partial\mathcal{B}} ds u(s) \partial_{\hat{n}'} G_0(\vec{r}, \vec{r}', E), \quad (23)$$

where  $\vec{r} = \vec{r}(s)$ ,  $\vec{r}' = \vec{r}(s')$ ,  $\hat{n}'$  is the outward normal vector to  $\partial\mathcal{B}$  at point  $\vec{r}'$ ,  $\partial_{\hat{n}'}$  is the projection of the gradient onto  $\hat{n}'$ , and  $G_0(\vec{r}, \vec{r}', E) = -(i/4)H_0^{(1)}(k|\vec{r} - \vec{r}'|)$  is the free Green function. The integral relation (23) has non-vanishing solutions  $u(s)$  only if

$$\det(\hat{I} - \hat{Q}(k)) = 0, \quad (24)$$

where  $\hat{I}$  is the identity and  $\hat{Q}(k)$  is an integral operator which, when applied to the function  $u(s)$ , gives the r.h.s. of Eq. (23). The zeros of (24) are the exact quantum energies of the system and the oscillatory part  $\tilde{d}(k)$  of the level density can be expressed as

$$\tilde{d}(k) = -\frac{1}{\pi} \Im \frac{d}{dk} \ln \det(\hat{I} - \hat{Q}(k)) = \frac{1}{\pi} \Im \sum_{n=1}^{\infty} \frac{1}{n} \frac{d}{dk} [\text{Tr} \hat{Q}^n(k)], \quad (25)$$

with

$$\text{Tr} \hat{Q}^n(k) = (-2)^n \int_{\partial\mathcal{B}} ds_1 \dots ds_n \partial_{\hat{n}_1} G_0(\vec{r}_2, \vec{r}_1, E) \partial_{\hat{n}_2} G_0(\vec{r}_3, \vec{r}_2, E) \dots \partial_{\hat{n}_n} G_0(\vec{r}_1, \vec{r}_n, E). \quad (26)$$

For a system with a boundary  $\mathcal{B}$  that is smooth everywhere, the integrals in (26) can be evaluated in stationary phase approximation. In this way  $\text{Tr} \hat{Q}^n$  is expressed in terms of a sum of contributions arising from periodic orbits with  $n$  specular reflections. Inserting this approximation into Eq. (25) yields Gutzwiller's trace formula as shown, for example, in Appendix B.

The standard approach described above is not convenient for deriving contributions of diffractive orbits, since the diffractive effects of the corners are hidden in this formulation. Instead, we use a

modification of the boundary element method by formulating it in terms of a Green function accounting for the diffractive effects of a corner.

We restrict to the consideration of diffractive orbits with a single corner point which are not influenced by the other corners of the billiard. To obtain the contribution of such an orbit to the trace formula it suffices to include the diffractive effect of only one corner. We further restrict in this section to corners in which the limit of the curvature of the boundary is zero when the corner is approached from either side. Modifications caused by non-vanishing curvature are discussed in Appendix D.

Let us first consider a simple billiard system which is bounded by a wedge of angle  $\gamma$  and an additional smooth curve  $C$  which connects the two sides of the wedge (such as represented in Fig. 6 for instance). One can derive an integral equation in terms of the Green function  $G_\gamma$  of the infinite wedge – analogous to equation (23) – in which the integration is restricted to the curve  $C$ . The oscillatory part of the spectral density is then again given by (25) where the trace of  $\hat{Q}^n$  now has the form

$$\text{Tr } \hat{Q}^n(k) = (-2)^n \int_C ds_1 \dots ds_n \partial_{\hat{n}_1} G_\gamma(\vec{r}_2, \vec{r}_1, E) \partial_{\hat{n}_2} G_\gamma(\vec{r}_3, \vec{r}_2, E) \dots \partial_{\hat{n}_n} G_\gamma(\vec{r}_1, \vec{r}_n, E). \quad (27)$$

Note that similar techniques have been used in Ref. [7] for deriving diffractive contributions in the Sinai billiard and in Ref. [31] for reformulating Fredholm's theory in the case of triangles.

The Green function  $G_\gamma$  can be split into a geometrical and a diffractive part as has been done in section 2

$$G_\gamma(\vec{r}, \vec{r}', E) = G_{geo}(\vec{r}, \vec{r}', E) + G_{diff}(\vec{r}, \vec{r}', E), \quad (28)$$

where the diffractive Green function is given by expressions (6,12,13). Inserting Eq. (28) into (27) results in  $2^n$  integrals. The stationary points of these integrals correspond to periodic and diffractive orbits of the billiard system (and possibly also to ghost orbits as in the case of billiards without corners), and the number of points in a corner of a diffractive orbit is determined by the number of diffractive parts  $G_{diff}$  appearing in the integral. Since we restrict to orbits with one point in a corner we can replace  $(n-1)$  of the Green functions in (27) by their geometrical part. This can be done in  $n$  ways which cancels the factor  $1/n$  in (25). Then the contribution to the level density from orbits with  $n$  reflections on the boundary  $C$  and one point in a corner are contained in

$$\tilde{d}_1^{(n)}(k) = \frac{(-2)^n}{\pi} \Im \frac{d}{dk} \int_C ds_1 \dots ds_n \partial_{\hat{n}_1} G_\gamma(\vec{r}_2, \vec{r}_1, E) \partial_{\hat{n}_2} G_{geo}(\vec{r}_3, \vec{r}_2, E) \dots \partial_{\hat{n}_n} G_{geo}(\vec{r}_1, \vec{r}_n, E), \quad (29)$$

an example is given in Fig. 5.

Let us discuss Eq. (29) in more detail. The contribution of a diffractive orbit is obtained by evaluating the integrals in the vicinity of the stationary points, i.e. in the vicinity of the points of specular reflection of the orbit on the boundary. If one approximates  $G_\gamma$  in the framework of GTD this results in Eq. (22) (with  $p=1$ ) for the contribution of the diffractive orbit. In the following we will improve on this method by using a uniform approximation for the Green function  $G_\gamma$ . In both cases however, only local information about the reflection points and the corner enters the approximation. It is then obvious how the expression (29) has to be modified in order to derive the semiclassical (or

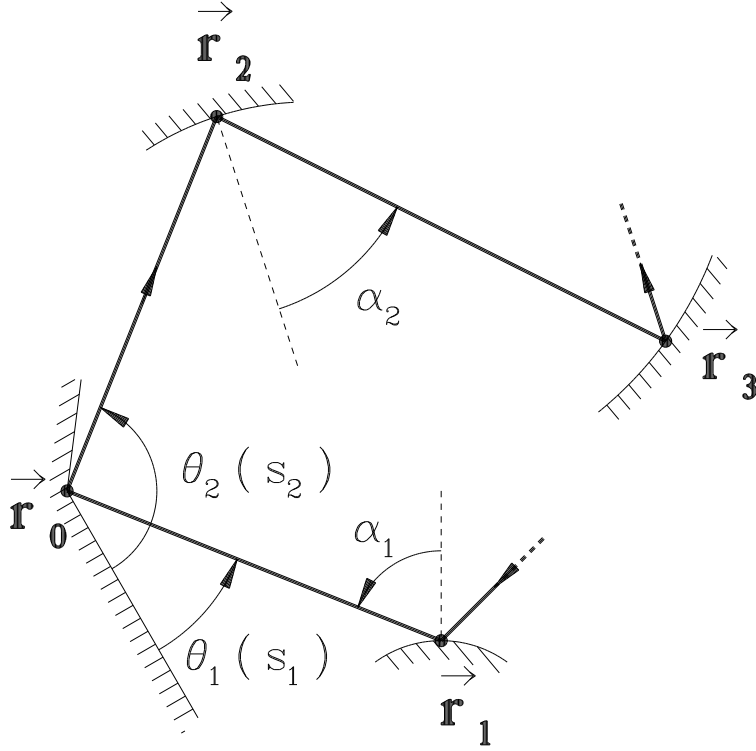


Figure 5: Typical path contributing to (29). A precise definition of the angles  $\alpha_i$  can be found in Appendix B.

uniform) contributions to  $d(k)$  for more complicated diffractive orbits in billiards with several corners: for every straight part between two reflection points a free Green function has to be included, and for every part of the trajectory which hits a corner between two reflections a Green function for an infinite wedge with the same angle. The reason why  $G_{geo}$  is appearing in Eq. (29) and not  $G_0$  is that in the above formulation we consider only reflections on the part  $C$  of the boundary, and  $G_{geo}$  takes care of the reflections on the wedge part. Hence the total number of specular reflections on  $\partial\mathcal{B}$  in Eq. (29) may be greater than  $n$ .

We continue now with the further evaluation of Eq. (29) which we perform in the case  $n \neq 1$ . The calculations for  $n = 1$  can be treated by identical methods and yield the same final result.

In (29),  $(n - 2)$  boundary integrals can be evaluated by applying the composition law (B1) for Green functions which is derived in Appendix B:

$$\partial_{\hat{n}_2} G_{sc}(\vec{r}_1, \vec{r}_2, E) \approx (-2)^{(n-2)} \int_C ds_3 \dots ds_n \partial_{\hat{n}_2} G_{geo}(\vec{r}_3, \vec{r}_2, E) \dots \partial_{\hat{n}_n} G_{geo}(\vec{r}_1, \vec{r}_n, E), \quad (30)$$

and consequently

$$\tilde{d}_1^{(n)}(k) = \frac{(-2)^2}{\pi} \Im \frac{d}{dk} \int_C ds_1 ds_2 \partial_{\hat{n}_1} G_\gamma(\vec{r}_2, \vec{r}_1, E) \partial_{\hat{n}_2} G_{sc}(\vec{r}_1, \vec{r}_2, E). \quad (31)$$

Here  $G_{sc}$  is the contribution to the semiclassical Green function from trajectories with  $(n - 2)$  reflections on the boundary curve  $C$  (and possibly further reflections on the wedge part of the boundary):

$$G_{sc}(\vec{r}_1, \vec{r}_2, E) = \sum_\xi \frac{1}{\sqrt{8\pi k |m_{12}|}} \exp\{ikl - i\frac{\pi}{2}\tilde{\nu} - i\frac{3\pi}{4}\}, \quad (32)$$

where  $m$  is the stability matrix (see Appendix B) and  $l$  the length of the classical orbit going from  $\vec{r}_2$  to  $\vec{r}_1$ .  $\tilde{\nu}$  is the number of conjugate points plus twice the number of specular reflections on the boundary. We use here  $\tilde{\nu}$  and lower case letters for  $m$  and  $l$  in order to distinguish these quantities from those of the whole diffractive orbit. The normal derivative of the Green function is given in leading order by

$$\partial_{\hat{n}_2} G_{sc}(\vec{r}_1, \vec{r}_2, E) \approx ik \cos \alpha_2 G_{sc}(\vec{r}_1, \vec{r}_2, E), \quad (33)$$

where  $\alpha_2$  is the outgoing reflection angle at  $\vec{r}_2$  (see Fig. 5).

In the following, we will consider the contributions of the geometrical and diffractive parts  $G_{geo}$  and  $G_{diff}$  to the Green function  $G_\gamma$  in Eq. (31) separately. As discussed above, the geometrical part will yield the contributions of periodic orbits. The reason why it has to be included also for the derivation of the contributions of diffractive orbits is that both  $G_{diff}$  and  $G_{geo}$  are discontinuous at the optical boundary (see the discussion in Sec. 2). For that reason the boundary contribution of  $G_{geo}$  which arises from this discontinuity has to be included in order to cancel the analogous contribution of  $G_{diff}$ .

### 3.1 The diffractive contribution

From (6,7,12,13) the diffractive part of the Green function  $G_\gamma$  can be approximated by

$$G_{diff}(\vec{r}_2, \vec{r}_1, E) \approx \sum_{\sigma, \eta = \pm 1} \sigma \eta \sqrt{\frac{2}{\pi k}} \frac{e^{-i\pi/4}}{16\gamma} \int_{-i\infty}^{i\infty} dz \frac{\exp\{ik\sqrt{r_1^2 + r_2^2 - 2r_1 r_2 \cos z}\}}{(r_1^2 + r_2^2 - 2r_1 r_2 \cos z)^{1/4} \tan\left(\frac{z + \phi_\sigma + \eta\pi}{2N}\right)}, \quad (34)$$

where  $r_1$  (resp.  $r_2$ ) is the distance from  $\vec{r}_1$  (resp.  $\vec{r}_2$ ) to the diffractive point, and  $\phi_\sigma = \theta_1 - \sigma\theta_2$  (see Fig. 5). Similarly to (33), the normal derivative  $\partial_{\hat{n}_1}$  yields a factor  $ik \cos \alpha_1$ . We insert (34) and one contribution  $\xi$  from (32) into (31) and consider the contribution from the vicinity of a stationary point which is chosen as origin of the  $s$ -variables. The main contribution to the  $z$ -integral comes from values near  $z = 0$  and the exponent is expanded in  $z$  up to second order

$$d_{\xi, diff}(k) \approx \frac{(-2)^2}{\pi} \Im \frac{d}{dk} \sum_{\sigma, \eta = \pm 1} \sigma \eta \sqrt{\frac{2}{\pi k}} \frac{e^{-i\pi/4}}{16\gamma} \frac{\exp\{-i\frac{\pi}{2}\tilde{\nu} - i\frac{3\pi}{4}\}}{\sqrt{8\pi k |m_{12}|}} (ik)^2 \cos \alpha_1 \cos \alpha_2$$

$$\int_C ds_1 ds_2 \int_{-i\infty}^{i\infty} dz \frac{\exp\{ik(l(s_1, s_2) + r_1(s_1) + r_2(s_2) - \frac{r_1 r_2}{2(r_1 + r_2)} z^2)\}}{\sqrt{r_1 + r_2} \tan\left(\frac{z + \phi_\sigma + \eta\pi}{2N}\right)}, \quad (35)$$

where the index  $\xi$  labels the diffractive orbit. A stationary phase approximation of all integrals would yield the contribution of the diffractive orbit in the GTD approximation. This approximation diverges at an optical boundary. In order to obtain a finite uniform approximation the effect of the nearest pole to  $z = 0$  has to be included. We treat this pole again by the method of Pauli

$$\begin{aligned} \frac{1}{\tan\left(\frac{z + \phi_\sigma + \eta\pi}{2N}\right)} &= \frac{1}{\tan\left(\frac{z + \phi_\sigma + \eta\pi}{2N}\right)} \frac{a_{\sigma,\eta} + \eta\sqrt{2} \sin \frac{z + \Delta\phi_\sigma}{2}}{a_{\sigma,\eta} + \eta\sqrt{2} \sin \frac{z + \Delta\phi_\sigma}{2}} \\ &\approx \frac{1}{\tan\left(\frac{\phi_{\sigma,0} + \eta\pi}{2N}\right)} \frac{a_{\sigma,\eta}}{a_{\sigma,\eta} + \eta \frac{z + \Delta\phi_\sigma}{\sqrt{2}}}, \end{aligned} \quad (36)$$

where  $\phi_{\sigma,0}$  is the value of  $\phi_\sigma$  at the stationary point,  $\Delta\phi_\sigma = \phi_\sigma - \phi_{\sigma,0}$  and  $a_{\sigma,\eta}$  is evaluated using (14) at the stationary point. Inserting (36) into (35) we obtain

$$\begin{aligned} d_{\xi,diff}(k) &\approx \Im \frac{d}{dk} \sum_{\sigma,\eta=\pm 1} \sigma \eta \frac{k \cos \alpha_1 \cos \alpha_2 \exp\{-i\frac{\pi}{2}\tilde{\nu}\}}{8\pi^2 \gamma \sqrt{(r_1 + r_2)} |m_{12}|} \frac{a_{\sigma,\eta}}{\tan\left(\frac{\phi_{\sigma,0} + \eta\pi}{2N}\right)} \\ &\int_{-\infty}^{\infty} ds_1 ds_2 \int_{-i\infty}^{i\infty} dz \frac{\exp\{ik(l(s_1, s_2) + r_1(s_1) + r_2(s_2) - \frac{r_1 r_2}{2(r_1 + r_2)} z^2)\}}{a_{\sigma,\eta} + \eta(z + \Delta\phi_\sigma)/\sqrt{2}}. \end{aligned} \quad (37)$$

The quantities  $l(s_1, s_2)$ ,  $r_1(s_1)$  and  $r_2(s_2)$  are now expanded up to second order in  $s_1$  and  $s_2$ . The expansion coefficients can be obtained from (B8). Furthermore we expand  $\Delta\phi_\sigma$  up to first order in  $s_1$  and  $s_2$ :  $\Delta\phi_\sigma(s_1, s_2) \approx s_1 \cos \alpha_1 / r_1 - \sigma s_2 \cos \alpha_2 / r_2$ . After a substitution

$$s_1 \rightarrow -\eta \frac{\sqrt{2}}{\cos \alpha_1} s_1, \quad s_2 \rightarrow -\eta \frac{\sqrt{2}}{\cos \alpha_2} s_2, \quad z \rightarrow -\eta \sqrt{2} z, \quad (38)$$

we obtain the following expression

$$\begin{aligned} d_{\xi,diff}(k) &\approx -\Im \frac{d}{dk} \sum_{\sigma,\eta=\pm 1} \sigma \eta \frac{k \exp\{-i\frac{\pi}{2}\tilde{\nu}\}}{\pi^2 \gamma \sqrt{8(r_1 + r_2)} |m_{12}|} \frac{a_{\sigma,\eta}}{\tan\left(\frac{\phi_{\sigma,0} + \eta\pi}{2N}\right)} \\ &\int_{-\infty}^{\infty} ds_1 ds_2 \int_{-i\infty}^{i\infty} dz \frac{\exp\{ik(l + r_1 + r_2 + a' s_1^2 + b' s_2^2 + \frac{2}{m_{12}} s_1 s_2 - cz^2)\}}{z + \frac{s_1}{r_1} - \sigma \frac{s_2}{r_2} - a_{\sigma,\eta}}, \end{aligned} \quad (39)$$

where

$$a' = \frac{m_{11}}{m_{12}} - \frac{2}{R_1 \cos \alpha_1} + \frac{1}{r_1}, \quad b' = \frac{m_{22}}{m_{12}} - \frac{2}{R_2 \cos \alpha_2} + \frac{1}{r_2}, \quad c = \frac{r_1 r_2}{r_1 + r_2}. \quad (40)$$



Here the quantities  $r_1$ ,  $r_2$  and  $l$  without argument denote the values at the stationary point. The derivative with respect to  $k$  in (39) yields in leading order a factor  $iL$  where  $L = r_1 + r_2 + l$  is the length of the diffractive orbit. In the next step we simplify the integrals by applying a transformation of the  $s$  variables such that the denominator of the integrand depends only on one of the new  $s$  variables

$$s = \frac{s_1}{r_1} - \sigma \frac{s_2}{r_2}, \quad s' = d r_2 s_1 + (1 - \sigma d) r_1 s_2. \quad (41)$$

The form of  $s'$  is chosen such that the Jacobian of the transformation is one and the value of  $d$  is determined by the requirement that the exponent in the integrand has no mixed quadratic term  $s's$ . The evaluations are done with Maple and result in

$$d_{\xi,diff}(k) \approx -\Re \sum_{\sigma,\eta=\pm 1} \sigma \eta \frac{kL \exp\{ikL - i\frac{\pi}{2}\tilde{\nu}\}}{\pi^2 \gamma \sqrt{8(r_1 + r_2)} |m_{12}| \tan\left(\frac{\phi_{\sigma,0} + \eta\pi}{2N}\right)} \frac{a_{\sigma,\eta}}{\int_{-\infty}^{\infty} ds ds' \int_{-\infty}^{\infty} dz \frac{\exp\{ik(as^2 + bs'^2 - cz^2)\}}{z + s - a_{\sigma,\eta}}}, \quad (42)$$

where

$$a = \frac{M_{12}c}{M_{12} - c(\text{Tr } M - \sigma 2)}, \quad b = \frac{M_{12} - c(\text{Tr } M - \sigma 2)}{m_{12}r_1r_2c}, \quad (43)$$

$$d = \frac{c(\sigma r_1 R_1 \cos \alpha_1 m_{11} - 2\sigma r_1 m_{12} + \sigma R_1 \cos \alpha_1 m_{12} + r_2 R_1 \cos \alpha_1)}{r_2 R_1 \cos \alpha_1 [M_{12} - c(\text{Tr } M - \sigma 2)]},$$

$M$  is the stability matrix of the diffractive orbit, i. e. the stability matrix of the classical trajectory starting from the corner going through  $\vec{r}_2$  and  $\vec{r}_1$  and back to the corner. There is a relation between  $\tilde{\nu}$ , the signs of  $a$  and  $b$  and the Maslov index  $\nu$  of the diffractive orbit

$$\exp\{-i\frac{\pi}{2}\tilde{\nu} + i\frac{\pi}{4}\sigma_a + i\frac{\pi}{4}\sigma_b\} = i \exp\{-i\frac{\pi}{2}\nu\}, \quad (44)$$

where  $\sigma_a = \text{sign}(a)$ ,  $\sigma_b = \text{sign}(b)$ . Hence  $\nu$  is equal to  $\tilde{\nu}$  plus the number of negative signs of  $a$  and  $b$  (modulo 4). This can be seen, for example, by evaluating the  $s_1$ - and  $s_2$ -integrals in Eq. (39) by the stationary phase method. Then from the composition law of Green functions the Maslov index  $\nu$  of the whole diffractive orbit is obtained by successive applications of (B12). Since a stationary phase approximation after the transformation (41) has to yield the same result, relation (44) follows immediately.

The integral over  $s'$  can now be evaluated, and the double integral over  $s$  and  $z$  is calculated in Appendix C (Eq. (C9)). The result is

$$d_{\xi,diff}(k) \approx -\Re \sum_{\sigma,\eta=\pm 1} \sigma \eta \tau_{\sigma} \frac{L \exp\{ikL - i\frac{\pi}{2}\tilde{\nu}\}}{\gamma \sqrt{8(r_1 + r_2)} |m_{12}b(a-c)| \tan\left(\frac{\phi_{\sigma,0} + \eta\pi}{2N}\right)} \frac{|a_{\sigma,\eta}|}{\exp\{-\frac{ikaca_{\sigma,\eta}^2}{a-c}\}} \left[ \text{erfc}\{aa_{\sigma,\eta} \sqrt{\frac{k}{i(a-c)}}\} - \text{erfc}\{|a_{\sigma,\eta}| \sqrt{\frac{kac}{i(a-c)}}\} \right], \quad (45)$$

where  $\tau_\sigma = \text{sign}(ac/(a-c)) = \text{sign}(M_{12}/(\text{Tr } M - \sigma 2))$ . As will be seen in the following section, the first error function in (45) is the contribution from the discontinuity of  $G_{diff}$  which is cancelled by the corresponding contribution from  $G_{geo}$ .

### 3.2 The geometrical contribution

For a given  $\sigma$  and  $\eta$  the geometrical orbit that corresponds to the nearest pole arises when  $\phi_\sigma - 2n_{\sigma,\eta}\gamma = -\eta\pi$  and it exists if  $\eta(2n_{\sigma,\eta}\gamma - \phi_\sigma) < \pi$ . This can be re-expressed in the form

$$a_{\sigma,\eta} = \sqrt{2} \cos\left(\frac{\phi_{\sigma,0} - 2n_{\sigma,\eta}\gamma}{2}\right) > -\sqrt{2} \sin \frac{\eta\Delta\phi_\sigma}{2} \approx -\frac{\eta\Delta\phi_\sigma}{\sqrt{2}}. \quad (46)$$

In the following we derive the contribution from the discontinuity of  $G_{geo}$ . For that purpose we apply exactly the same approximations to  $G_{geo}$  that were used for  $G_{diff}$ . This is done by writing  $G_{geo}$  in the form

$$\begin{aligned} G_{geo}(\vec{r}_2, \vec{r}_1, E) &\approx - \sum_{\sigma,\eta=\pm 1} \sigma \Theta(A) \sqrt{\frac{2}{\pi k}} \frac{e^{i\pi/4}}{4} \frac{\exp\{ik\sqrt{r_1^2 + r_2^2 - 2r_1r_2 \cos(\phi_\sigma - 2n_{\sigma,\eta}\gamma)}\}}{(r_1^2 + r_2^2 - 2r_1r_2 \cos(\phi_\sigma - 2n_{\sigma,\eta}\gamma))^{1/4}} \quad (47) \\ &= - \sum_{\sigma,\eta=\pm 1} \sigma \Theta(A) \sqrt{\frac{2}{\pi k}} \frac{e^{-i\pi/4}}{16\gamma} \oint dz \frac{\exp\{ik\sqrt{r_1^2 + r_2^2 - 2r_1r_2 \cos z}\}}{(r_1^2 + r_2^2 - 2r_1r_2 \cos z)^{1/4} \tan\left(\frac{z + \phi_\sigma + \eta\pi}{2N}\right)}, \end{aligned}$$

where  $A = a_{\sigma,\eta} + \sqrt{2} \sin(\eta\Delta\phi_\sigma/2)$ . The integration contour of the  $z$ -integral encircles the nearest pole to  $z = 0$  counter-clockwise. The expression (47) differs from Eq. (34) only by a factor  $(-\eta)$ , the  $\Theta$ -function and the integration contour. We repeat now all the steps from Eq. (35) to (42). The only difference is an multiplicative factor  $(-\eta)$  which results from the substitution  $z \rightarrow -\eta\sqrt{2}z$  (it didn't appear previously because of the different integration contour). We arrive at an expression corresponding to Eq. (42)

$$\begin{aligned} &-\Re \sum_{\sigma,\eta=\pm 1} \sigma \eta \frac{kL \exp\{ikL - i\frac{\pi}{2}\tilde{\nu}\}}{\pi^2 \gamma \sqrt{8(r_1 + r_2)} |m_{12}|} \frac{a_{\sigma,\eta}}{\tan\left(\frac{\phi_{\sigma,0} + \eta\pi}{2N}\right)} \\ &\int_{-\infty}^{\infty} ds ds' \oint dz \Theta(a_{\sigma,\eta} - s) \frac{\exp\{ik(as^2 + bs'^2 - cz^2)\}}{z + s - a_{\sigma,\eta}}. \quad (48) \end{aligned}$$

The triple integral is denoted by  $I$ . The integrals over  $s'$  and  $z$  can now be evaluated and result in

$$\begin{aligned} I &= 2\pi i \sqrt{\frac{\pi i}{kb}} \int_{-\infty}^{a_{\sigma,\eta}} ds \exp\{ikas^2 - ikc(s - a_{\sigma,\eta})^2\} \\ &= 2\pi i \sqrt{\frac{\pi i}{kb}} \int_{-\infty}^0 ds \exp\{ik(a-c)(s + \frac{aa_{\sigma,\eta}}{a-c})^2 - i\frac{kaca^2_{\sigma,\eta}}{a-c}\}. \quad (49) \end{aligned}$$

We are interested only in the boundary contribution of the geometrical part. The expression (48) contains in general also contributions from periodic orbits. This is the case if the integration range in (49) contains a stationary point, i. e. if  $aa_{\sigma,\eta}/(a-c)$  is positive. Then the stationary point contribution has to be subtracted which corresponds to a subtraction of the integral from  $-\infty$  to  $\infty$ . We obtain for the boundary contribution

$$\begin{aligned} I' &= -\text{sign}(a_{\sigma,\eta}) \tau_{\sigma} 2\pi i \sqrt{\frac{\pi i}{kb}} \int_0^{\infty} ds \exp\left\{ik(a-c)\left(s + \left|\frac{aa_{\sigma,\eta}}{a-c}\right|\right)^2 - i\frac{kaca_{\sigma,\eta}^2}{a-c}\right\} \\ &= -\text{sign}(a_{\sigma,\eta}) \tau_{\sigma} \frac{\pi^2}{k} \frac{1}{\sqrt{|b(a-c)|}} e^{i\frac{\pi}{4}(1+\sigma_a+\sigma_b+\tau_{\sigma})} \exp\left\{-i\frac{kaca_{\sigma,\eta}^2}{a-c}\right\} \text{erfc}\left\{|aa_{\sigma,\eta}| \sqrt{\frac{k}{i(a-c)}}\right\}, \end{aligned} \quad (50)$$

where  $\tau_{\sigma} = \text{sign}(ac/(a-c))$ , as before. Substituting  $I'$  for the triple integral in (48) yields

$$\begin{aligned} d_{\xi,geo}(k) &\approx \Re \sum_{\sigma,\eta=\pm 1} \sigma\eta\tau_{\sigma} \frac{L \exp\{ikL - i\frac{\pi}{2}\tilde{\nu}\}}{\gamma\sqrt{8(r_1+r_2)}|m_{12}b(a-c)|} \frac{|a_{\sigma,\eta}|}{\tan\left(\frac{\phi_{\sigma,0} + \eta\pi}{2N}\right)} \\ &\quad e^{i\frac{\pi}{4}(1+\sigma_a+\sigma_b+\tau_{\sigma})} \exp\left\{-\frac{kaca_{\sigma,\eta}^2}{a-c}\right\} \text{erfc}\left\{|aa_{\sigma,\eta}| \sqrt{\frac{k}{i(a-c)}}\right\}. \end{aligned} \quad (51)$$

Comparison with Eq. (45) shows that this contribution exactly cancels the first error function in (45).

### 3.3 The joint contribution

We now can write down the final formula of this section. By using the definitions of  $a$ ,  $b$  and  $c$  the sum of (45) and (51) can be written in the form

$$\begin{aligned} d_{\xi}(k) &\approx -\Re \sum_{\sigma,\eta=\pm 1} \eta\tau_{\sigma} \frac{L}{\pi} \frac{\exp\{ikL - i\frac{\pi}{2}\mu_{\sigma}\}}{\sqrt{|\text{Tr } M - \sigma 2|}} \frac{|a_{\sigma,\eta}|}{2N\sqrt{2} \tan\left(\frac{\phi_{\sigma} + \eta\pi}{2N}\right)} \\ &\quad \exp\left\{-\frac{ika_{\sigma,\eta}^2 M_{12}}{\text{Tr } M - \sigma 2}\right\} \text{erfc}\left\{|a_{\sigma,\eta}| \sqrt{\frac{kM_{12}}{i(\text{Tr } M - \sigma 2)}}\right\}, \end{aligned} \quad (52)$$

where we dropped the second index of  $\phi_{\sigma,0}$  for simplicity of notation. Furthermore,  $\mu_{\sigma} = \nu + (1-\sigma) + \kappa_{\sigma}$ ,  $\tau_{\sigma} = 1 - 2\kappa_{\sigma}$ , and  $\kappa_{\sigma}$  is defined as

$$\kappa_{\sigma} = \begin{cases} 0 & \text{if } \frac{M_{12}}{\text{Tr } M - \sigma 2} > 0, \\ 1 & \text{if } \frac{M_{12}}{\text{Tr } M - \sigma 2} < 0. \end{cases} \quad (53)$$

We recall that  $M$  in (52,53) is the stability matrix (at unit energy) of the classical trajectory starting and ending at the corner point.  $\nu$  is the number of conjugate points of this trajectory, plus

2 times the number of specular reflections. The definition of  $\mu_\sigma$  in terms of  $\nu$  and  $\kappa_\sigma$  is similar to the definition of the Maslov index of a periodic orbit in terms of that of the Green function [33]. The  $\sigma$ -dependence is due to the fact that positive  $\sigma$  values are associated with geometrical orbits that are reflected an even number of times near the corner, as an optical boundary is approached, and negative  $\sigma$  values with orbits with an odd number of bounces. This is explained in more detail in Appendix D. In the limiting case that the diffractive orbit becomes a periodic orbit, its contribution comes only from one of the values of  $\sigma$  (the other cancels), and its stability matrix is  $M$  or  $-M$  depending on whether the number of bounces of the orbit in the corner is even or odd (cf. the discussion in 4.2). Thus  $\mu_\sigma$  is identical to the Maslov index of the periodic orbit in these limiting cases.

In terms of the Fresnel integral  $K$  formula (52) can be written in a slightly shorter form

$$d_\xi(k) \approx -\Re \sum_{\sigma, \eta = \pm 1} \eta \tau_\sigma \frac{L}{\pi} \frac{\exp\{ikL - i\frac{\pi}{2}\mu_\sigma\}}{\sqrt{|\text{Tr } M - \sigma 2|}} \frac{|a_{\sigma, \eta}|}{N\sqrt{2} \tan\left(\frac{\phi_\sigma + \eta\pi}{2N}\right)} K\left(|a_{\sigma, \eta}| i^{\kappa_\sigma} \sqrt{\frac{k|M_{12}|}{|\text{Tr } M - \sigma 2|}}\right). \quad (54)$$

Equation (54) is the main result of this paper. It gives a uniform approximation for the contribution of an isolated diffractive orbit with a single corner point to the trace formula. For completeness we recall several definitions:  $\phi_\sigma = \theta_1 - \sigma\theta_2$ , where  $\theta_1$  and  $\theta_2$  are the incoming and outgoing angles at the diffractive point (measured from the same edge, with  $\theta_1$  and  $\theta_2 \in [0, \gamma]$ ) and  $a_{\sigma, \eta}$  is defined by

$$a_{\sigma, \eta} = \sqrt{2} \cos\left(\frac{\phi_\sigma}{2} - n_{\sigma, \eta}\gamma\right) \quad \text{with} \quad n_{\sigma, \eta} = \text{nint}\left[\frac{\phi_\sigma + \eta\pi}{2\gamma}\right] \in \mathbb{Z}. \quad (55)$$

Note finally that the modified Fresnel function of imaginary argument (encountered when  $\kappa_\sigma = 1$ ) can be computed numerically from (A3).

## 4 Discussion of the result

In this section we discuss properties and the range of validity of formula (54). As mentioned above, the derivation has been done for a specific case (a wedge connected to a smooth boundary), but it is more generally valid because it relies only on local properties of the system near the considered diffractive orbit (as usual in semiclassical approximations). Hence it applies to billiards of any shape provided the singularity of the boundary corresponds locally to the intersection of two straight lines. However, the present approach has to be refined if applied to curved edges, we discuss this point in Appendix D. We also remind that formula (54) is only valid for single diffraction. The same formalism can in principle also be applied to diffractive orbits with more than one diffractive point, the formulas become however increasingly more complex. For example, in the case of double diffraction, one has already 16 instead of 4 terms, and they involve also double Fresnel integrals as can be inferred from the treatment of diffraction at two wedges in [21]. The formulas can only be simplified if the diffraction in some of the corners can be treated in the GTD approximation.

Note also, that the factor  $|\text{Tr } M - 2\sigma|^{-1/2}$  in (54) diverges for a parabolic diffractive orbit (i. e. when  $\text{Tr } M = \pm 2$ ) and the present approach cannot be used in this case. This is very similar to divergences in Gutzwiller's trace formula due to non-isolated orbits. For diffractive orbits, the fact that  $\text{Tr } M = \pm 2$  can have several reasons, for example the diffractive orbits can appear in families as

is the case in a circular sector, or bifurcations of diffractive orbits can occur, or the diffractive orbit can become a part of a family of periodic orbits when the optical boundary is approached. The latter case can occur for example in triangular billiards. In this case it is however often possible to treat the divergent part (one of the  $\sigma$ -values) in the GTD approximation if the diffractive orbit is well separated from the torus of periodic orbits, and apply the uniform approximation only to the non-divergent part as will be demonstrated in a numerical example in section 5.

#### 4.1 The GTD limit

After these basic remarks we now study three simple limits of Eq. (54). The first one is the geometrical theory of diffraction which is valid sufficiently far away from the optical boundary. In this limit the argument of the  $K$  function is large and the function can be replaced by its leading asymptotic term in (A4). This immediately yields

$$d_\xi(k) \approx \frac{L}{\pi} \frac{\mathcal{D}(\theta_1, \theta_2)}{\sqrt{8\pi k |M_{12}|}} \cos(kL - \nu\pi/2 - 3\pi/4), \quad (56)$$

which agrees with the general formula (22) in the case of one diffractive point. Analogous formulae have been derived and tested in [4, 6, 8]. They have the advantage of allowing to treat general diffractive problems (other than wedge diffraction) and can easily be generalized to multiple diffraction (see (22)). However they diverge on the optical boundary and (as shown in the examples 5.1 and 5.2 below) they are unable to describe the limit that a diffractive orbit is close to become a real trajectory.

#### 4.2 The limit $\gamma = \pi/p$

Let us now study the limit that the diffraction angle  $\gamma$  goes to  $\pi/p$  ( $p \in \mathbb{N}^*$ ). For these values of  $\gamma$  there is no diffraction since the corner can be treated by the method of images. As a consequence, the contributions of most diffractive orbits disappear, but there are also diffractive orbits which are replaced by periodic orbits which contribute to the level density according to Gutzwiller trace formula. Their contribution can be obtained from the diffractive contribution (54) in the limit  $\gamma \rightarrow \pi/p$ . The situation is actually slightly more complicated, since the diffractive contribution of these orbits for angles  $\gamma = \pi/p + \epsilon$  is discontinuous at  $\epsilon = 0$  (it changes sign). The reason for this is that periodic orbits split from the diffractive orbit as  $\epsilon$  goes through zero (for example as the billiard is deformed), which can be considered as a kind of bifurcation. As a consequence both diffractive and periodic orbit contributions are discontinuous at  $\epsilon = 0$ , but their sum remains continuous. In order to discuss this in more detail we have to consider the cases of odd and even  $p$  separately.

- Case  $\gamma = \frac{\pi}{2p} + \epsilon$ . In the limit  $\epsilon = 0$  the contributions from the two  $\eta$ -values cancel for  $\sigma = -1$ . The same occurs for  $\sigma = +1$ , except if  $\theta_2 = \theta_1$ . If this condition is fulfilled one obtains

$$d_\xi(k) \rightarrow \text{sign}(\epsilon) \tau_{(+)} d_{po}(k), \quad (57)$$

where

$$d_{po}(k) = \frac{L}{\pi} \frac{\cos(kL - \mu_{(+)}\pi/2)}{|\text{Tr } M - 2|^{1/2}} \quad \left( \text{when } \gamma = \frac{\pi}{2p} \right). \quad (58)$$

The discontinuity in Eq. (57) at  $\epsilon = 0$  is directly related to the appearance of new periodic orbits. This can be seen from the discussion in section 3.2: in Eq. (49) one has contributions of periodic orbits in the vicinity of the diffractive orbit if  $a_{\sigma,\eta}\tau_\sigma > 0$ , and the periodic orbits coincide with the diffractive orbit when  $a_{\sigma,\eta} = 0$ . For the considered case the above inequality is equivalent to  $-\text{sign}(\epsilon)\tau_+ > 0$ . Hence when  $\epsilon$  goes through zero, two periodic orbits appear (or disappear), one for each value of  $\eta$ , assuring the continuity of the sum of contributions at  $\epsilon = 0$ .

- Case  $\gamma = \pi/(2p+1) + \epsilon$ . Now the two contributions to  $\sigma = +1$  cancel as  $\epsilon \rightarrow 0$ , and for  $\sigma = -1$  there is only a contribution if  $\theta_2 = \gamma - \theta_1$ . This contribution is of the form

$$d_\xi(k) \rightarrow \text{sign}(\epsilon) \tau_{(-)} d_{po}(k), \quad (59)$$

and the periodic orbit contribution now is given by

$$d_{po}(k) = \frac{L}{\pi} \frac{\cos(kL - \mu_{(-)}\pi/2)}{|\text{Tr } M + 2|^{1/2}} \quad \left( \text{when } \gamma = \frac{\pi}{2p+1} \right). \quad (60)$$

Comparing with (58), the reason for the change of sign of  $M$  is the odd number of classical reflections on the vertex in the case  $\gamma = \pi/(2p+1)$ . Generally, the stability matrix  $M$  of the closed trajectory in (54) becomes equal to plus (resp. minus) the monodromy matrix of the periodic orbit when  $\gamma$  is  $\pi/(2p)$  (resp.  $\pi/(2p+1)$ ). The explanation of the discontinuity of Eq. (59) is the same as above with the only difference that the condition for the existence of neighbouring periodic orbits can now be expressed by  $-\text{sign}(\epsilon)\tau_- > 0$ .

In billiards with corners one has therefore a new kind of bifurcation: the continuity of wave mechanics (in the semiclassical approximation) is not enforced by complex trajectories but by diffractive orbits. This effect will be demonstrated in the examples below.

### 4.3 In the vicinity of an optical boundary

The case that a diffractive orbit lies on an optical boundary, or crosses an optical boundary when the billiard is deformed, is very similar to the case  $\gamma \rightarrow \pi/p$ . Again the diffractive orbit contributes on the optical boundary at the same order of  $k$  as a periodic orbit, but now only with half the amplitude of a periodic orbit. The diffractive contribution is again discontinuous since it changes sign as an optical boundary is crossed, and the reason for this is that a new periodic orbit arises which bifurcates from the diffractive orbit. More specifically, let us consider the case that for a given value of  $\sigma$  and  $\eta$  one has  $\phi_\sigma - 2n_{\sigma,\eta}\gamma + \eta\pi = \epsilon$  where  $\epsilon$  is small. In the limit  $\epsilon \rightarrow 0$  the contribution from these values of  $\sigma$  and  $\eta$  to the spectral density is given by

$$-\frac{1}{2} \eta \tau_\sigma \text{sign}(\epsilon) d_{po}(k) \quad \text{where} \quad d_{po}(k) = \frac{L}{\pi} \frac{\cos(kL - \mu_\sigma \pi/2)}{\sqrt{|\text{Tr } M - 2\sigma|}}. \quad (61)$$

and one can verify that the discontinuity of Eq. (61) is due to a neighbouring periodic orbit which coincides with the diffractive orbit at  $\epsilon = 0$ . As above, the condition for the existence of the periodic orbit is  $a_{\sigma,\eta}\tau_\sigma > 0$  which now is equivalent to  $\eta\epsilon\tau_\sigma > 0$ .

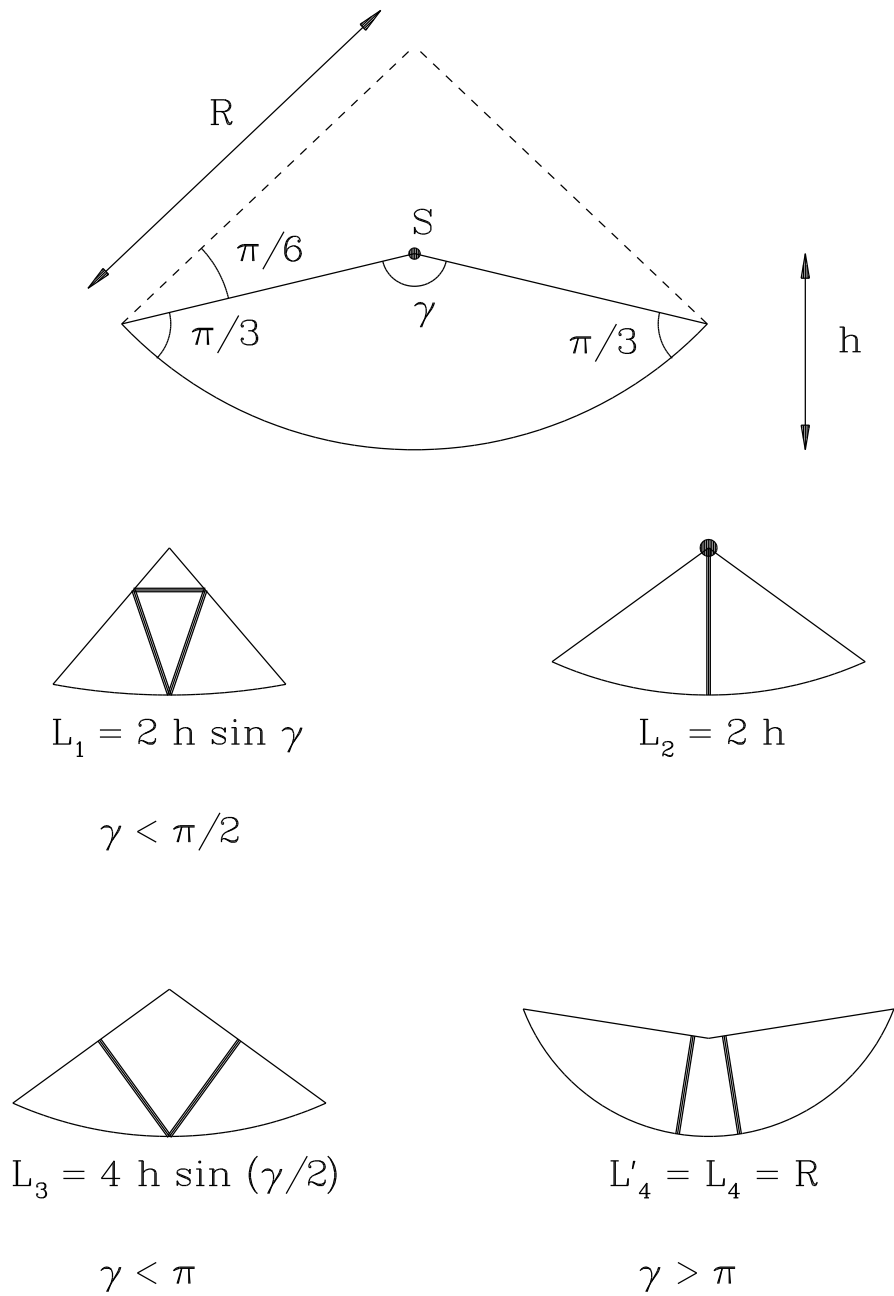


Figure 6: Shortest periodic and diffractive orbits in the “rounded triangular billiard” studied in Sec. 5. For the diffractive orbit, the diffractive point is marked with a black point. The upper plot defines the geometry and the notations.

## 5 Some examples

In this section we illustrate the results of the last sections with several examples. We study mainly a billiard consisting of a wedge of opening angle  $\gamma$  whose two edges are connected by an arc of constant radius of curvature  $R$ . The angles between arc and wedge are chosen to be  $\pi/3$  on both sides. If  $h$  denotes the “height” of this billiard (see Fig. 6) then  $R = h \sin(\gamma/2)(\sin(\gamma/2) - 1/2)^{-1}$ . This billiard has only one diffractive corner (at point  $S$  of Fig. 6) and the curvature ensures that the shortest diffractive and periodic orbits have  $\text{Tr } M \neq \pm 2$  (they are displayed in Fig. 6). In the following we call this billiard a “rounded triangle ( $\pi/3, \pi/3, \gamma$ )”.

For numerical convenience we restrict ourselves to angles of the form  $\gamma = p\pi/q$  with  $(p, q) \in \mathbb{N}^2$ . The quantum energies are determined by expanding the wave functions around point  $S$  in “partial waves” which are Bessel functions times a sinusoidal function of the angle:

$$\psi(r, \theta) = \sum_{n=1}^{n_{max}} J_{nq/p}(kr) \sin\left(\frac{nq}{p}\theta\right). \quad (62)$$

Eq. (62) automatically fulfills the Dirichlet condition on the straight faces of the billiard. The boundary condition on the arc opposite to  $S$  is enforced in a manner identical to the improved point matching method presented in [32]. This results in a secular equation whose solutions are the eigen levels of the system. We have tested the numerical stability of our procedure by varying the number  $n_{max}$  of partial waves included in the expansion (typically  $n_{max} \approx \text{rint}[pkh/q]$ ). For each of the values of  $\gamma$  studied below we have computed the first 2000 eigenlevels and we have checked that they were determined with an accuracy of the order of 1/1000 of the mean level spacing.

In order to visualize the importance of periodic and diffractive orbits we study in the following the regularized Fourier transform of the level density:

$$F(x) = \int_0^{k_{max}} \sqrt{k} e^{ikx - \alpha k^2} d(k) dk. \quad (63)$$

$k_{max}$  is the last eigenvalue computed numerically and we take here  $\alpha = 10/k_{max}^2$ . The multiplicative factor  $\sqrt{k}$  in (63) is included in order to cancel the singularity at  $k = 0$  of a contribution of type (56).  $F(x)$  is denoted  $F_{QM}(x)$  if we use in (63) the exact quantum spectrum. It is denoted  $F_{UA}(x)$  (resp.  $F_{CTD}(x)$ ) when Eq. (54) (resp. (56)) is used together with the periodic orbit contributions (B21).

### 5.1 $\gamma$ near $\pi/2$

This case is relevant to the discussion 4.2 above. For  $\gamma < \pi/2$  the shortest orbit is a periodic one and has length  $L_1 = 2h \sin \gamma$ . It disappears as soon as  $\gamma > \pi/2$ . For  $\gamma \neq \pi/2$  one also has a diffractive orbit of length  $L_2 = 2h$  (see Fig. 6). When  $\gamma = \pi/2$  these orbits coalesce and give a single periodic orbit of length  $2h$ . Their contribution to the level density is continuous at  $\gamma = \pi/2$  as explained above: the contribution of  $L_2$  is discontinuous (cf. Eq. (57)) and this exactly cancels the discontinuity due to the disappearance of the orbit  $L_1$  and its time reverse.

We determined the spectrum numerically for  $\gamma = 7\pi/15$  and  $8\pi/15$ . The corresponding moduli of the Fourier transform  $|F(x)|$  are plotted in Fig. 7 and 8. In this figures the solid lines correspond



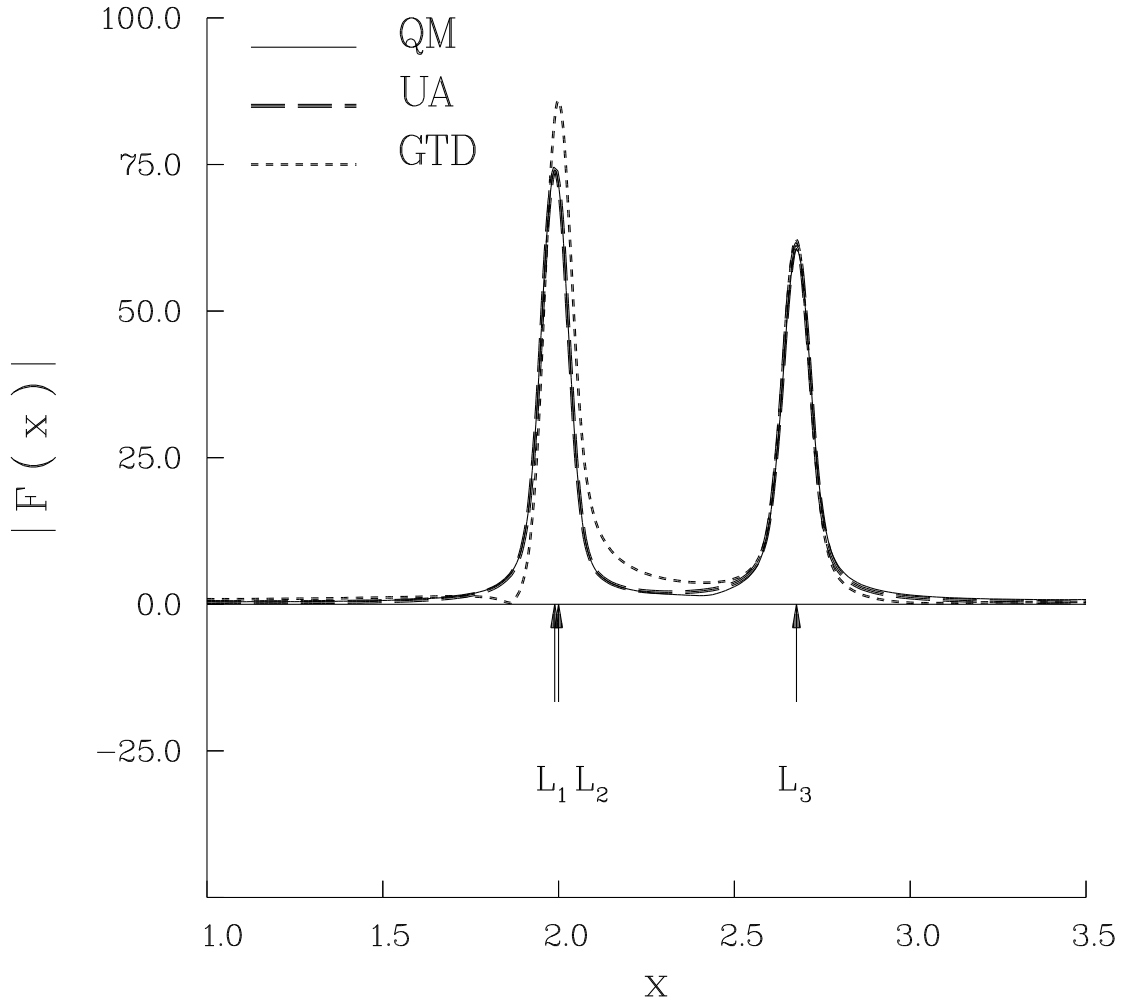


Figure 7: Modulus  $|F(x)|$  of the Fourier transform of the level density – see Eq. (63) – for the rounded triangle  $(\pi/3, \pi/3, \gamma = 7\pi/15)$ . The solid line corresponds to  $F_{QM}(x)$ , the long dashed line to  $F_{UA}(x)$  and the short dashed line to  $F_{GTD}(x)$  (see the text). The arrows mark the lengths of the diffractive and periodic orbits. The scale of lengths and wave-vectors is fixed by taking  $h = 1$ .

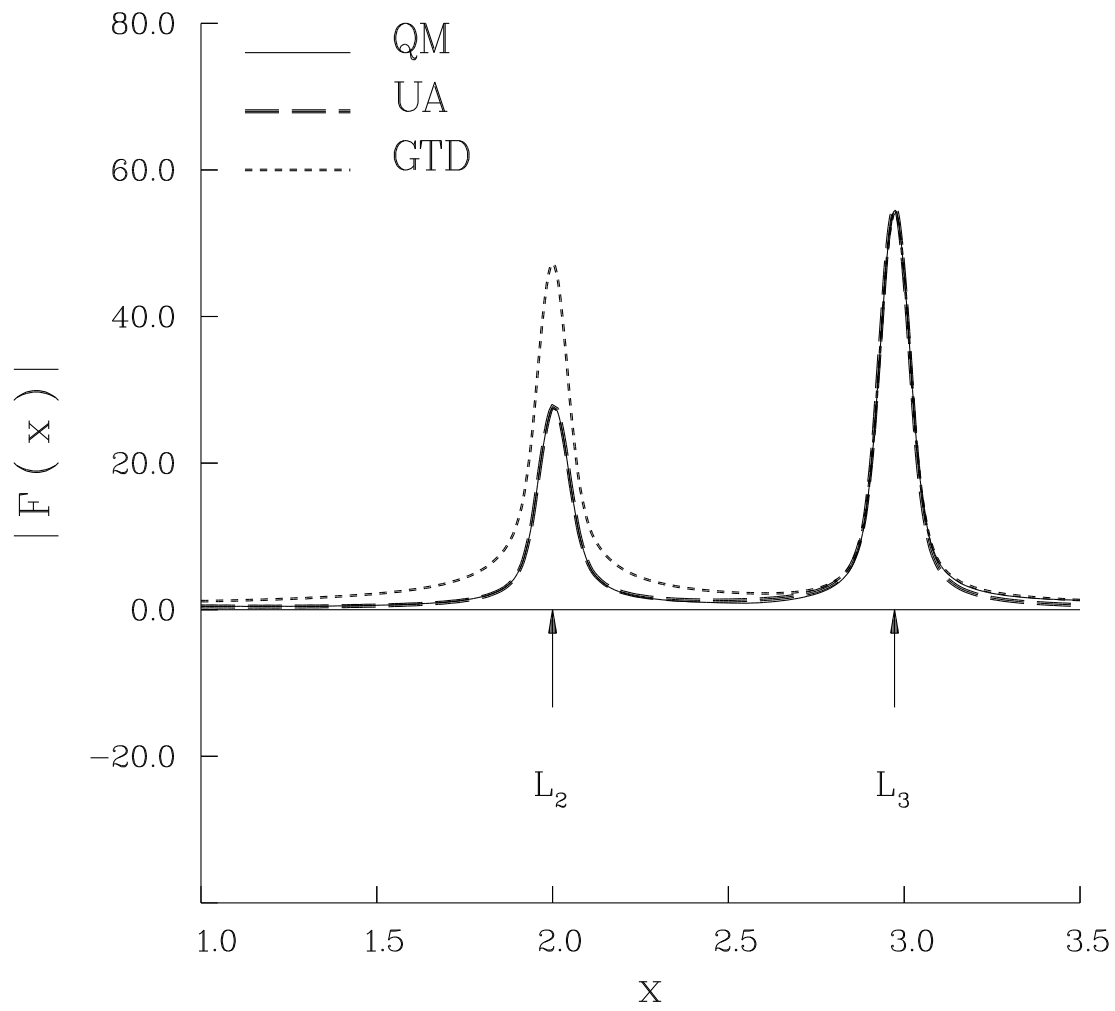


Figure 8: Same as Fig. 7 for  $\gamma = 8\pi/15$ .

to  $|F_{QM}(x)|$ , the long dashed lines to  $|F_{UA}(x)|$  and the short dashed line to  $|F_{GTD}(x)|$ . The lengths of the included orbits are marked with back arrows. One notices the failure of GTD and the excellent agreement of approximation (54) with the exact result (the agreement remains equally good when plotting the real and imaginary part of  $F(x)$ ). As stated above, it can be seen that in the vicinity of an optical boundary diffractive and periodic orbits contribute in the same order to the level density.

## 5.2 $\gamma$ near $\pi$

This case also pertains to the discussion of Sec. 4.2, but now in the vicinity of  $\gamma = \pi/(2p + 1)$ . Again the diffractive orbit ensures continuity of semiclassical mechanics when  $\gamma = \pi$ : the two periodic orbits  $L_4$  and  $L'_4$  of Fig. 6 disappear as soon as  $\gamma < \pi$ , and the contribution of  $L_2$  is discontinuous at  $\gamma = \pi$ , but the joint contribution is continuous. Here we computed numerically the levels for  $\gamma = 19\pi/20$  and present the results for  $|F(x)|$  and  $\Re\{F(x)\}$  in Fig. 9. Again one can verify the failure of the geometrical theory of diffraction and the excellent agreement between (54) and the quantum result.

## 5.3 The triangle $(\pi/4, \pi/6, 7\pi/12)$

In this subsection we depart from the previous examples and study the spectrum of a straight triangular billiard with angles  $(\pi/4, \pi/6, 7\pi/12)$  which has one diffractive wedge  $\gamma = 7\pi/12$ . This billiard is of interest because (i) it allows to compare the performances of the uniform approximation with GTD in a regime where this last approximation is not inaccurate and also (ii) because it provides an example where our approach is not completely justified. Indeed in case of a polygonal billiard all the trajectories have a monodromy matrix with  $\text{Tr } M = \pm 2$  and this leads to a divergence in (54). As noted in Sec. 4 this is linked to the possible deformation of any diffractive orbit of the system considered towards a family of periodic orbits. Fortunately, in the present case the first diffractive orbits are far from any allowed family of periodic orbits and we can evaluate the  $K$ -function relevant to the divergent term in (54) with the asymptotic expansion (A4): this cancels the divergence. This was done on Fig. 10 for the 3 first diffractive orbits of the system.

Again the agreement with the numerical result is excellent, but here the geometrical theory of diffraction already gives a sensible description. Note however that the small peak due to the diffractive boundary orbit of length  $L_2$  is “missed” by GTD because its diffractive coefficient (10) is zero (see the discussion in 2.2). The correct description of the peak was obtained by using half the contribution (54) of a usual diffractive orbit.

For a more detailed comparison we plot the moduli of the differences  $|F_{UA}(x) - F_{QM}(x)|$  and  $|F_{GTD}(x) - F_{QM}(x)|$  in figure 11: even quite far from any optical boundary Eq. (54) supersedes the GTD result (56). This plot emphasizes the accuracy of Eq. (54) in cases slightly out of its original range of application.

## 6 Conclusion

In this paper we have studied the inclusion of diffractive orbits in semiclassical trace formulae for billiards in which the boundary has wedge-like singularities. In many cases the simple geometrical theory of diffraction [9] is inadequate, especially if the energy is not very high. A consideration of the mathematical structure of the exact Green function near a wedge permits to remedy this

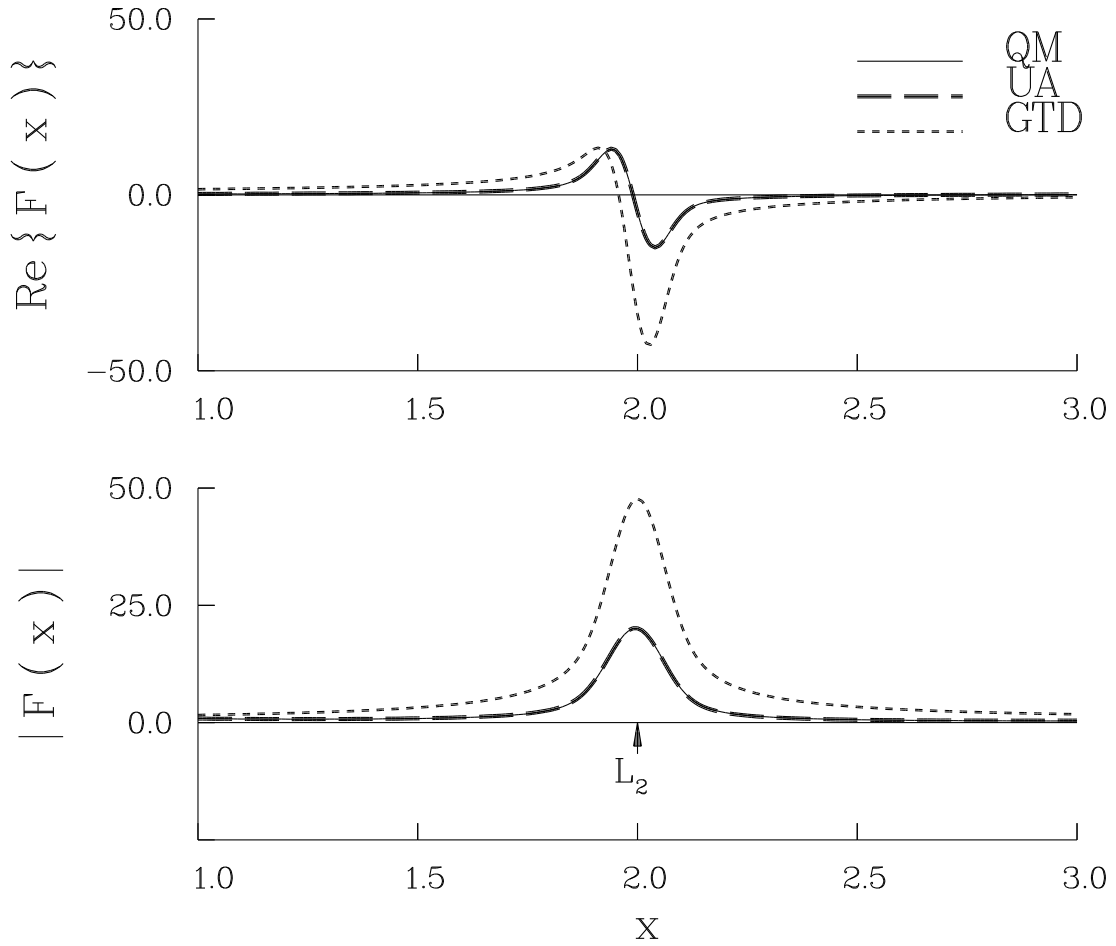


Figure 9: Same as Fig. 7 for  $\gamma = 19\pi/20$ . We plot here also  $\Re\{F(x)\}$  for illustrating the quality of the agreement between the phases of  $F_{QM}$  and  $F_{UA}$ .

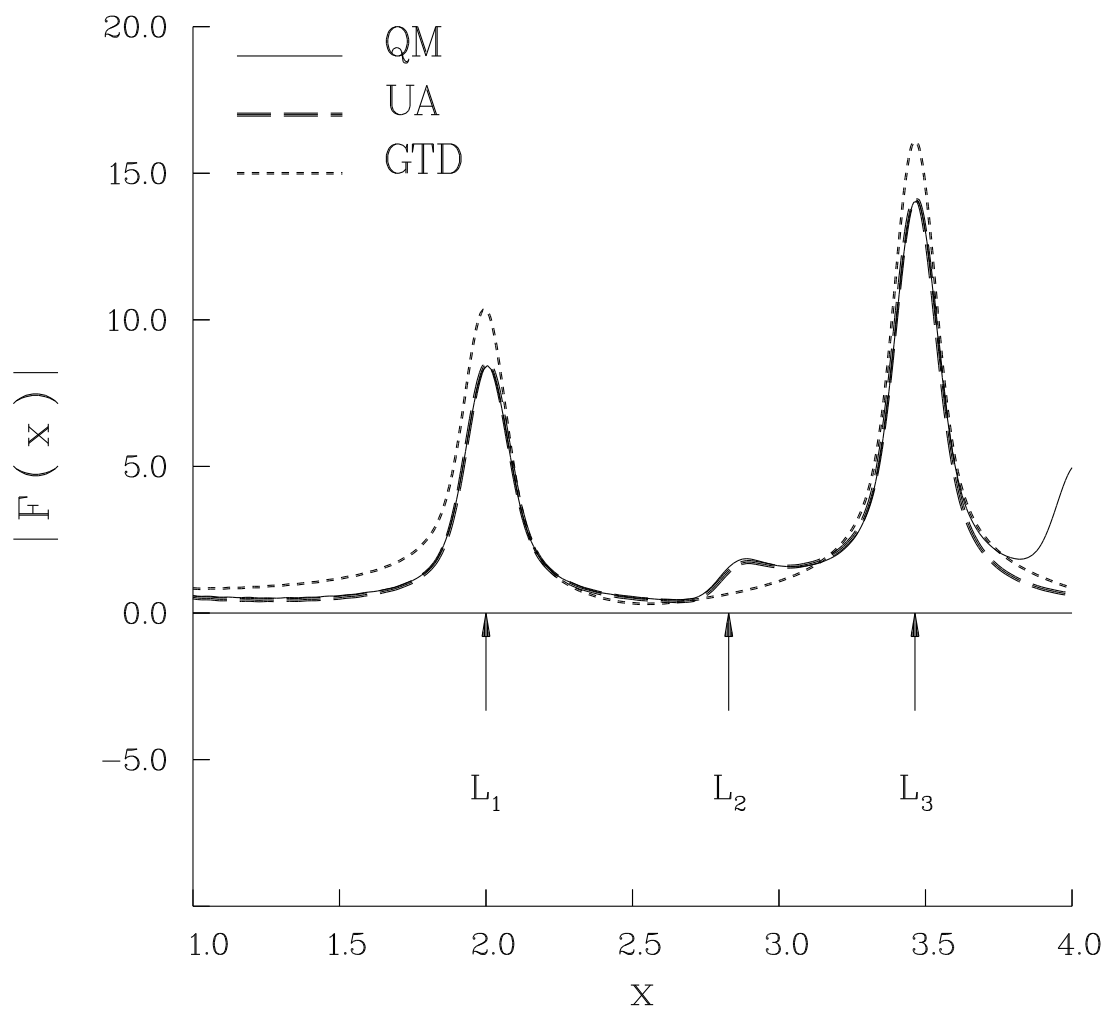
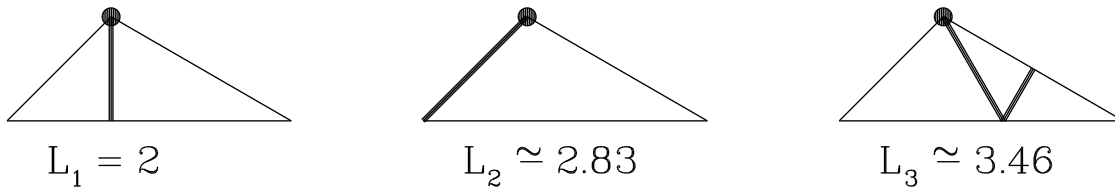


Figure 10: Same as Fig. 7 for the flat triangle  $(\pi/4, \pi/6, 7\pi/12)$ . The upper part displays the shortest orbits of the system (all three are diffractive, the classical periodic orbits occur at greater lengths).

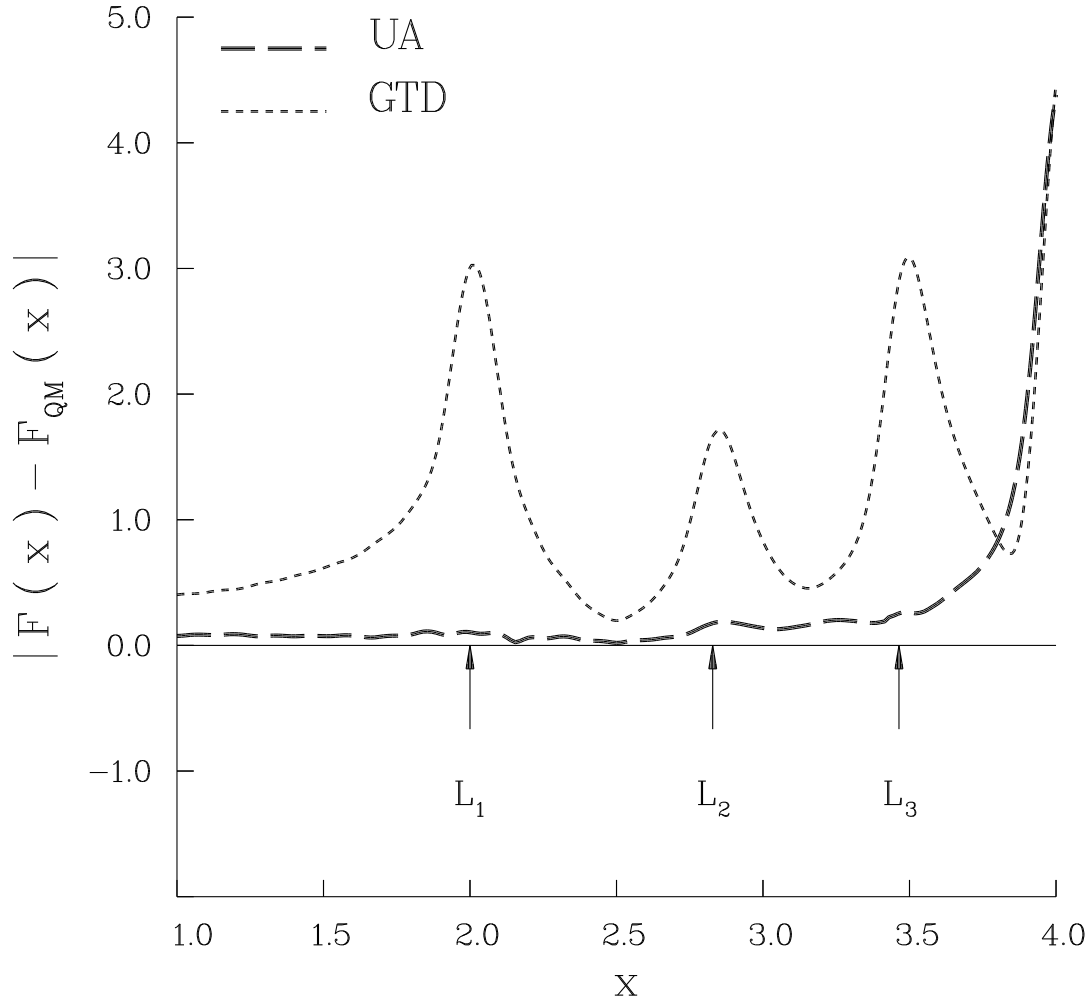


Figure 11:  $|F_{UA}(x) - F_{QM}(x)|$  (long dashed line) and  $|F_{GTD}(x) - F_{QM}(x)|$  (short dashed line) for the triangle  $(\pi/4, \pi/6, 7\pi/12)$ . We consider only the three shortest orbits of the system. The following orbits are not taken into account and this is the reason for the increasing errors in vicinity of  $x \approx 4$ .

shortcoming: it leads to a uniform approximation of the Green function [16] which, in turn, allows to derive contributions to the trace formula which properly account for the role of isolated diffractive orbits in the quantum spectrum (54). The formula was illustrated in several examples and was shown to give excellent agreement with numerical data. Its main feature is that it interpolates between the usual Gutzwiller trace formula [1] and previous approaches relying on the geometrical theory of diffraction [4, 6, 8].

Note also – as a by-product of the present approach – that we derived a semiclassical composition law for Green functions for billiard systems (B1,B13) reminiscent to the semigroup composition property of the propagator (see the discussion in [1]). This allows to recover Gutzwiller’s trace formula in a simple fashion (cf. Appendix B). Similar laws can also be obtained for the composition of diffractive and geometrical Green functions.

The present work suggests further developments: (i) the result (54) might be extended to allow the treatment of diffractive orbits in the vicinity of a family of periodic orbits; (ii) although the inclusion of general multiple diffraction in a uniform formula seems to be a difficult task, one may reasonably hope to include double diffraction in the formalism (cf. [21]). (iii) Further possible extensions concern the treatment of other types of diffraction, like regions near curved wedges where surface diffraction becomes important so that contributions from creeping and whispering gallery orbits have to be included, or diffraction effects arising from discontinuities of the curvature of the boundary like in the stadium billiard.

Finally we would like to emphasize the important role of diffraction in semiclassical approaches. Diffractive and periodic orbits are fundamentally different in the sense that the former are not obtained via a systematic  $\hbar$  expansion in the vicinity of classical solutions of Hamilton’s equations (they are rather linked to discontinuities of the Hamiltonian flow). However diffractive orbits provide the first correction to the leading order in the trace formula, with contributions typically of order  $\sqrt{\hbar}$  smaller than the contributions of isolated periodic orbits. Besides, in the vicinity of optical boundaries the two types of orbit contribute with approximately the same order to the trace formula. An image emerging from our study (cf. Sec. 4.2 and 4.3) is that diffractive orbits allow to enforce semiclassically the continuity of wave mechanics in the vicinity of discontinuities or bifurcations of classical mechanics.

## Acknowledgments

M. S. acknowledges financial support by the Alexander von Humboldt-Stiftung and by the Deutsche Forschungsgemeinschaft under contract No. DFG-Ste 241/7-1. La Division de Physique Théorique de l’Institut de Physique Nucléaire est une unité de recherche des universités Paris XI et Paris VI associée au CNRS.

## Appendix A The modified Fresnel function

In this Appendix we define the modified Fresnel function  $K(z)$  used in the main text and list several of its properties.

- The function  $K(z)$  ( $z \in \mathbb{C}$ ) is defined by:

$$K(z) = \frac{e^{-i(z^2 + \pi/4)}}{\sqrt{\pi}} \int_z^\infty e^{iy^2} dy = \frac{e^{-iz^2}}{2} \operatorname{erfc}(e^{-i\pi/4}z), \quad (\text{A1})$$

where  $\operatorname{erfc}$  is the complementary error function (see e.g. [25]). In (A1) the path of integration is subject to the restriction  $\arg(y) \rightarrow \alpha$  with  $0 < \alpha < \pi/2$  as  $y \rightarrow \infty$  along the path.  $\alpha = 0$  and  $\pi/2$  are permissible if  $\operatorname{Re}(iy^2)$  remains bounded to the right.

The function  $K$  has the following properties:  $K(+\infty) = 0$ ,  $K(0) = 1/2$ ,

$$K(z) + K(-z) = e^{-iz^2}, \quad (\text{A2})$$

and

$$\overline{K(\bar{z})} + K(-iz) = e^{iz^2}, \quad (\text{A3})$$

where the bar denotes complex conjugation.

- By successive integrations by parts one obtains the following asymptotic expansion:

$$K(z) = \frac{e^{i\pi/4}}{2z\sqrt{\pi}} \sum_{n=0}^{+\infty} \left(\frac{1}{2}\right)_n \left(\frac{-i}{z^2}\right)^n \quad \text{for } |z| \rightarrow +\infty \quad \text{and} \quad -\pi/4 < \arg(z) < 3\pi/4, \quad (\text{A4})$$

where  $(1/2)_n = \Gamma(n+1/2)/\Gamma(1/2) = 1 \times 3 \times \dots \times (2n-1)/2^n$ . In the region  $\arg(z) \in ]3\pi/4, 7\pi/4[$  one obtains an asymptotic expansion by combining Eqs. (A2) and (A4).

- The interest in the modified Fresnel function comes from the following integral relation:

$$\int_{-\infty}^{+\infty} dt \frac{e^{-\beta t^2}}{t-z} = 2i\tau\pi K\left(\tau e^{-i\pi/4}\sqrt{\beta}z\right), \quad (\text{A5})$$

where  $\beta \in \mathbb{R}^+$ ,  $z \in \mathbb{C}$  and  $\tau = \operatorname{sign}(\Im(z))$ .

Hence the function  $K$  allows to generalize the steepest descent method to cases where poles appear in the integrand. As explained in the text (Sec. 2) this corresponds – in the Sommerfeld solution of the diffraction problem – to the occurrence of diffractive orbits near classical trajectories. We will not prove Eq. (A5) here, it can be done easily by noting that  $(t-z)^{-1} = i\tau \int_0^{+\infty} \exp[i\tau(z-t)x] dx$  (cf. the evaluation of integral (C6) in Appendix C).

## Appendix B Composition law for Green functions

In this Appendix we derive a simple semiclassical composition law for Green functions which is expressed by integrals over the boundary  $\partial\mathcal{B}$  of the billiard. Although the formulae established below are simple and natural from the point of view of Balian and Bloch's multiple reflexion expansion [2], to our knowledge they have not been clearly stated in the literature. The composition law can be used in order to simplify expressions obtained from the boundary element method (cf. (31)). We first prove



the semiclassical version and then give the exact formulation of this law due to Balian and Bloch. We further show that it allows to derive Gutzwiller's trace formula in a straightforward manner.

We assume in this Appendix that the boundary  $\partial\mathcal{B}$  is smooth everywhere. The semiclassical version of the composition law has the form

$$(-2)^n \int_{\partial\mathcal{B}} ds_1 \dots ds_n G_0(\vec{r}_1, \vec{r}', E) \partial_{\hat{n}_1} G_0(\vec{r}_2, \vec{r}_1, E) \dots \partial_{\hat{n}_n} G_0(\vec{r}, \vec{r}_n, E) \approx G_{sc}^{(n)}(\vec{r}, \vec{r}', E). \quad (\text{B1})$$

where  $\vec{r}_i = \vec{r}(s_i)$ . The approximate sign signifies that the evaluation is done by approximating the free Green function  $G_0$  by its leading asymptotic term for large argument and evaluating the integrals in stationary phase approximation. The function  $G_{sc}^{(n)}(\vec{r}, \vec{r}', E)$  on the right-hand side of Eq. (B1) is the part of the semiclassical Green function from all trajectories with  $n$  bounces on the boundary between  $\vec{r}'$  and  $\vec{r}$

$$G_{sc}^{(n)}(\vec{r}, \vec{r}', E) = \sum_{\xi_n} \frac{1}{\sqrt{8\pi k |M_{12}^{(n)}|}} \exp\{ikl^{(n)} - i\frac{\pi}{2}\nu^{(n)} - i\frac{3\pi}{4}\}. \quad (\text{B2})$$

Here  $l^{(n)}$  denotes the length of the trajectory,  $\nu^{(n)}$  is the number of conjugate points from  $\vec{r}'$  to  $\vec{r}$  plus twice the number of reflections on the boundary, and  $M^{(n)}$  is the stability matrix for unit energy. An index  $\xi_n$  of the above quantities has been omitted in order to simplify the notations.

Eq. (B1) is proven by mathematical induction. For  $n = 0$  it is correct since

$$G_0(\vec{r}, \vec{r}', E) \approx G_{sc}^{(0)}(\vec{r}, \vec{r}', E), \quad (\text{B3})$$

and one has to show that

$$I := (-2) \int_{\partial\mathcal{B}} ds_1 G_{sc}^{(n)}(\vec{r}_1, \vec{r}', E) \partial_{\hat{n}_1} G_0(\vec{r}, \vec{r}_1, E) \approx G_{sc}^{(n+1)}(\vec{r}, \vec{r}', E). \quad (\text{B4})$$

We will use the following notation at a point  $\vec{r}_i$  of the boundary: primed quantities correspond to the incoming trajectory and unprimed quantities to the outgoing trajectory. We will denote the momentum of a classical trajectory by a vector  $\vec{p}$  of modulus  $k$  whose direction is the direction of propagation of the classical particle. The momentum of an outgoing trajectory is  $\vec{p}_i$  and  $\alpha_i$  is the angle between the normal vector  $\hat{n}_i$  of the boundary (which points outside) and  $-\vec{p}_i$ . The momentum of an incoming trajectory is  $\vec{p}'_i$ , and  $\alpha'_i$  is the angle between  $\hat{n}_i$  and  $\vec{p}'_i$ . For this choice  $\alpha'_i$  and  $\alpha_i$  both lie in the interval between  $-\pi/2$  and  $\pi/2$ . In terms of the local coordinate systems of the trajectories with coordinates parallel and perpendicular to the trajectory, the tangential and normal vectors of the boundary can be written as:

$$\begin{aligned} \hat{n}_i &= -\cos \alpha_i \hat{e}_{\parallel} + \sin \alpha_i \hat{e}_{\perp} = \cos \alpha'_i \hat{e}'_{\parallel} - \sin \alpha'_i \hat{e}'_{\perp}, \\ \hat{t}_i &= -\sin \alpha_i \hat{e}_{\parallel} - \cos \alpha_i \hat{e}_{\perp} = \sin \alpha'_i \hat{e}'_{\parallel} + \cos \alpha'_i \hat{e}'_{\perp}. \end{aligned} \quad (\text{B5})$$

We continue by evaluating the integral in Eq. (B4) using the stationary phase approximation. The normal derivative of the Green function is given in leading semiclassical order by

$$\partial_{\hat{n}_i} G_0(\vec{r}_{i+1}, \vec{r}_i, E) \approx -i \hat{n}_i \cdot \vec{p}_i G_{sc}^{(0)}(\vec{r}_{i+1}, \vec{r}_i, E) = ik \cos \alpha_i G_{sc}^{(0)}(\vec{r}_{i+1}, \vec{r}_i, E), \quad (\text{B6})$$

and in (B4) the stationary points are determined by the condition

$$0 = \frac{d}{ds_1} [l^{(0)}(\vec{r}, \vec{r}_1) + l^{(n)}(\vec{r}_1, \vec{r}')] = \hat{t} \cdot \left[ -\frac{\vec{p}_1}{k} + \frac{\vec{p}_1'}{k} \right] = \sin \alpha_1 + \sin \alpha'_1, \quad (\text{B7})$$

i. e. by  $\alpha_1 = -\alpha'_1$ , which is the condition for elastic reflection. The sum over all stationary points thus expresses the integral  $I$  by a sum over all trajectories with  $n + 1$  reflections on the boundary. In Eq. (B7) and in the following the length is given two arguments when it is necessary to specify the starting and end point of the trajectory.

For the determination of the second derivatives of the lengths at a boundary point  $s_i$  one has to evaluate the derivatives of the angles  $\alpha_i$  and  $\alpha'_i$  which consist of two parts. One from the change of the normal vector with  $s_i$  and one from the change of the direction of the trajectories.

$$\begin{aligned} \frac{d^2 l^{(n)}(\vec{r}_i, \vec{r}_{i-1})}{ds_i^2} &= \cos \alpha'_i \frac{d\alpha'_i}{ds_i} = \cos \alpha'_i \left( -\frac{1}{R_i} + \frac{\cos \alpha'_i}{k} \frac{dp'_{i\perp}}{dq_{i\perp}} \right) = -\frac{\cos \alpha'_i}{R_i} + \frac{\cos^2 \alpha'_i M_{22}^{(n)}}{M_{12}^{(n)}}, \\ \frac{d^2 l^{(n)}(\vec{r}_{i+1}, \vec{r}_i)}{ds_i^2} &= \cos \alpha_i \frac{d\alpha_i}{ds_i} = \cos \alpha_i \left( -\frac{1}{R_i} - \frac{\cos \alpha_i}{k} \frac{dp_{i\perp}}{dq_{i\perp}} \right) = -\frac{\cos \alpha_i}{R_i} + \frac{\cos^2 \alpha_i M_{11}^{(n)}}{M_{12}^{(n)}}. \end{aligned} \quad (\text{B8})$$

At a stationary point it follows with these relations that

$$\frac{d^2}{ds_1^2} [l^{(0)}(\vec{r}, \vec{r}_1) + l^{(n)}(\vec{r}_1, \vec{r}')] = -\frac{\cos^2 \alpha_1 M_{12}^{(n+1)}}{M_{12}^{(0)} M_{12}^{(n)}}, \quad (\text{B9})$$

where  $M^{(n+1)} = M^{(0)} B_1 M^{(n)}$  and the matrices  $M^{(0)}$  and  $B_1$  are given by

$$M^{(0)} = \begin{pmatrix} 1 & l^{(0)} \\ 0 & 1 \end{pmatrix}, \quad B_1 = \begin{pmatrix} -1 & 0 \\ \frac{2}{R_1 \cos \alpha_1} & -1 \end{pmatrix}. \quad (\text{B10})$$

The matrices  $M$  and  $B$  correspond to the linearized flow near the considered trajectory. Note that our definition is slightly different from usual conventions (see e. g. [1, 33]): considering that here  $|\vec{p}| = k$ , the  $M_{12}$  (resp.  $M_{21}$ ) matrix element would be generally divided (resp. multiplied) by  $k$ . Here we work with the stability matrix at unit energy: this choice is connected to the scaling property of the dynamics in billiard systems. It does not affect the trace and the determinant of the matrix and allows to have energy independent matrix elements with a simple geometrical meaning.

Now the stationary phase approximation for the integral in Eq. (B4) is carried out and results in:

$$\begin{aligned} I &\approx \sum_{\xi_{n+1}} \frac{\cos \alpha_1 \exp\{ikl^{(n+1)} - i\frac{\pi}{2}\nu^{(n)}\}}{4\pi\sqrt{|M_{12}^{(0)} M_{12}^{(n)}|}} \int_{\partial\mathcal{B}} ds_1 \exp\left\{-ik\frac{\cos^2 \alpha_1 M_{12}^{(n+1)}}{2M_{12}^{(0)} M_{12}^{(n)}} s_1^2\right\} \\ &\approx \sum_{\xi_{n+1}} \frac{1}{\sqrt{8\pi k |M_{12}^{(n+1)}|}} \exp\left\{ikl^{(n+1)} - i\frac{\pi}{2}\nu^{(n+1)} - i\frac{3\pi}{4}\right\}, \end{aligned} \quad (\text{B11})$$

where  $l^{(n+1)} = l^{(0)} + l^{(n)}$  and

$$\nu^{(n+1)} = \nu^{(n)} + 2 + \begin{cases} 1 & \text{if } \text{sign}(M_{12}^{(n+1)}) = \text{sign}(M_{12}^{(n)}) , \\ 0 & \text{if } \text{sign}(M_{12}^{(n+1)}) \neq \text{sign}(M_{12}^{(n)}) . \end{cases} \quad (\text{B12})$$

Eq. (B12) coincides with the expected definition of the Maslov index:  $\nu^{(n+1)}$  is the number of conjugate points from  $\vec{r}'$  to  $\vec{r}$  plus twice the number of reflections on the boundary; an additional conjugate point has occurred between  $\vec{r}_1$  and  $\vec{r}$  iff  $\text{sign}(M_{12}^{(n+1)}) = \text{sign}(M_{12}^{(n)})$  (remember that there is one sign change due to the reflection on the boundary). This completes the proof of Eq. (B4) and thus also of Eq. (B1).

A further relation follows from the fact that the evaluation of the integral in Eq. (B1) does not depend on the order in which the stationary phase approximations are carried out. Thus one can conclude directly that

$$(-2) \int_{\partial\mathcal{B}} ds_1 G_{sc}^{(n)}(\vec{r}_1, \vec{r}', E) \partial_{\hat{n}_1} G_{sc}^{(m)}(\vec{r}, \vec{r}_1, E) \approx G_{sc}^{(n+m+1)}(\vec{r}, \vec{r}', E) . \quad (\text{B13})$$

Equations (B1) and (B13) were derived in the semiclassical approximation by evaluating the boundary integrals only locally in the vicinity of stationary points. For that reason the same composition law can be applied in order to obtain the contributions of the geometrical orbits in billiards with corners; this is done in Eq. (30).

We note that equations (B1) and (B13) are the semiclassical versions of *exact* relations for the Green function  $G$  of a billiard system. These exact relations are obtained by a multiple reflection expansion of the Green function  $G$  [2]:

$$G(\vec{r}, \vec{r}', E) = \sum_{n=0}^{\infty} G^{(n)}(\vec{r}, \vec{r}', E) , \quad (\text{B14})$$

where

$$G^{(n)}(\vec{r}, \vec{r}', E) = (-2)^n \int_{\partial\mathcal{B}} ds_1 \dots ds_n G_0(\vec{r}_1, \vec{r}', E) \partial_{\hat{n}_1} G_0(\vec{r}_2, \vec{r}_1, E) \dots \partial_{\hat{n}_n} G_0(\vec{r}, \vec{r}_n, E) , \quad (\text{B15})$$

and the equation analogous to (B13) follows directly.

Finally, we show that Gutzwiller's trace formula can be obtained in a straightforward way by using (B1). From the boundary element method one obtains

$$d(k) = \bar{d}(k) + \frac{1}{\pi} \Im \sum_{n=1}^{\infty} \frac{1}{n} \frac{d}{dk} \text{Tr} \hat{Q}^n(k) , \quad (\text{B16})$$

where

$$\text{Tr} \hat{Q}^n(k) = (-2)^n \int_{\partial\mathcal{B}} ds_1 \dots ds_n \partial_{\hat{n}_1} G_0(\vec{r}_2, \vec{r}_1, E) \partial_{\hat{n}_2} G_0(\vec{r}_3, \vec{r}_2, E) \dots \partial_{\hat{n}_n} G_0(\vec{r}_1, \vec{r}_n, E) . \quad (\text{B17})$$

With Eq. (B1) it follows that

$$\begin{aligned}
d(k) &\approx \bar{d}(k) - \frac{2}{\pi} \frac{d}{dk} \Im \sum_{n=1}^{\infty} \frac{1}{n} \int_{\partial \mathcal{B}} ds \partial_{\hat{n}'} G_{sc}^{(n-1)}(\vec{r}, \vec{r}', E)|_{\vec{r}=\vec{r}'} \\
&\approx \bar{d}(k) - \frac{2}{\pi} \Re \sum_{n=2}^{\infty} \frac{1}{n} \frac{k l^{(n-1)} \cos \alpha}{\sqrt{8\pi k |M_{12}^{(n)}|}} \int_{\partial \mathcal{B}} ds \exp\{ikl^{(n-1)}(\vec{r}, \vec{r}') - i\frac{\pi}{2}\nu^{(n-1)} - i\frac{\pi}{4}\}. \quad (\text{B18})
\end{aligned}$$

The stationary phase condition is again given by  $\sin \alpha = -\sin \alpha'$  and thus the integral yields contributions from periodic orbits with  $n$  specular reflections on the boundary. More accurately, it gives  $n/r_{po}$  (identical) contributions for every periodic orbit where  $r_{po}$  is the repetition number of the orbit, since there are  $n/r_{po}$  different starting positions  $\vec{r} = \vec{r}'$  on  $\partial \mathcal{B}$ .

The derivatives of the angles  $\alpha$  and  $\alpha'$  now have additional contributions since both initial and final points of the trajectory are changed by varying  $s$

$$\begin{aligned}
\frac{d\alpha'}{ds} &= -\frac{1}{R} + \frac{\cos \alpha'}{k} \frac{dp'_{\perp}}{dq'_{\perp}} \Big|_{q_{\perp}} - \frac{\cos \alpha}{k} \frac{dp_{\perp}}{dq_{\perp}} \Big|_{q'_{\perp}} = -\frac{1}{R} + \frac{\cos \alpha' M_{22}^{(n-1)} + \cos \alpha}{M_{12}^{(n-1)}}, \\
\frac{d\alpha}{ds} &= -\frac{1}{R} - \frac{\cos \alpha}{k} \frac{dp_{\perp}}{dq_{\perp}} \Big|_{q'_{\perp}} + \frac{\cos \alpha'}{k} \frac{dp'_{\perp}}{dq'_{\perp}} \Big|_{q_{\perp}} = -\frac{1}{R} + \frac{\cos \alpha M_{11}^{(n-1)} + \cos \alpha'}{M_{12}^{(n-1)}}. \quad (\text{B19})
\end{aligned}$$

It then follows at a stationary point that

$$\frac{d^2}{ds^2} l^{(n-1)}(\vec{r}, \vec{r}') = -\frac{\cos^2 \alpha (\text{Tr } M_{po}^{(n)} - 2)}{(M_{po}^{(n)})_{12}}, \quad (\text{B20})$$

where  $M_{po}^{(n)} = B_1 M^{(n-1)}$ .

and the stationary phase approximation results in

$$d(k) = \bar{d}(k) + \frac{1}{\pi} \sum_{n=1}^{\infty} \sum_{\xi_{n,po}} \frac{l_{po}^{(n)}}{r_{po} \sqrt{|\text{Tr } M_{po}^{(n)} - 2|}} \cos\{kl_{po}^{(n)} - \frac{\pi}{2}\mu_{po}^{(n)}\}, \quad (\text{B21})$$

where

$$\mu_{po}^{(n)} = \nu^{(n-1)} + 2 + \begin{cases} 0 & \text{if } (M_{po}^{(n)})_{12}/(\text{Tr } M_{po}^{(n)} - 2) > 0, \\ 1 & \text{if } (M_{po}^{(n)})_{12}/(\text{Tr } M_{po}^{(n)} - 2) < 0. \end{cases} \quad (\text{B22})$$

Note that the derivation presented here has the same starting point as Ref. [28]. But the composition law (B1) permits to bypass the computation of large determinants of [28]. Furthermore, it allows to keep track of the Maslov indices (which were not derived in [28]) in a simple way.

Finally we add a remark on ghost contributions. In general, the semiclassical approximation for the Green functions  $G^{(n)}(\vec{r}, \vec{r}', E)$  can also contain contributions from ghost trajectories that satisfy the stationary phase conditions but have parts that are outside the billiard region. These ghost orbits, however, do not give a contribution to the level density  $d(k)$  since they cancel with ghost contributions from different  $n$  or from  $\bar{d}(k)$  [3, 28, 29, 34].

## Appendix C Evaluation of a diffraction integral

In this appendix the integral

$$I = \int_{-\infty}^{\infty} ds \int_{-i\infty}^{i\infty} dz \frac{e^{ias^2 - icz^2}}{z + s - s_0}, \quad (\text{C1})$$

is evaluated for positive  $c$  and real non-vanishing  $a$  and  $s_0$ . This is the basic integral which appears in the derivation of the uniform approximation for diffractive contributions to the trace formula.

First the  $z$ -integral is rotated onto the real axis. The rotation is performed counter-clockwise: since  $c > 0$  this yields no contribution from infinity. There are, however, poles of the integrand on the real  $z$  line. We take them into account by giving to  $s_0$  a small imaginary part  $s_0 \rightarrow s_0 + i\sigma_0\varepsilon$  and consider the limit  $\varepsilon \rightarrow 0$  in the end. Here  $\sigma_0 = \text{sign}(s_0)$  and  $\varepsilon > 0$ . For this choice one obtains a pole contribution from the rotation of the  $z$ -integral for those values of  $s$  for which  $(s_0 - s)$  has a different sign than  $s_0$ . One obtains

$$\int_{-i\infty}^{i\infty} dz \frac{e^{-icz^2}}{z + s - s_0} = \lim_{\varepsilon \rightarrow 0} \int_{\infty}^{-\infty} dz \frac{e^{-icz^2}}{z + s - s_0 - i\sigma_0\varepsilon} + 2\pi i\sigma_0 e^{-ic(s - s_0)^2} \Theta(\sigma_0(s - s_0)). \quad (\text{C2})$$

We consider now the two contributions of the r.h.s. of Eq. (C2) to the integral in (C1) separately,  $I = I_0 + I_1$ , where  $I_0$  contains the pole contribution and  $I_1$  the contribution from the rotated  $z$ -integral. For  $I_0$  we have

$$\begin{aligned} I_0 &= 2\pi i\sigma_0 \int_{-\infty}^{\infty} ds \Theta(\sigma_0(s - s_0)) e^{ias^2 - ic(s - s_0)^2} \\ &= 2\pi i\sigma_0 \int_{|s_0|}^{\infty} ds e^{ias^2 - ic(s - |s_0|)^2} \\ &= \frac{i\pi\sqrt{\pi}\sigma_0}{\sqrt{-i(a-c)}} \exp\left\{-\frac{iacs_0^2}{a-c}\right\} \text{erfc}\left\{\frac{-ia|s_0|}{\sqrt{-i(a-c)}}\right\}, \end{aligned} \quad (\text{C3})$$

where  $\text{erfc}$  is the complementary error function (see e. g. [25]).  $I_1$  has the form

$$I_1 = -\lim_{\varepsilon \rightarrow 0} \int_{-\infty}^{\infty} ds \int_{-\infty}^{\infty} dz \frac{e^{ias^2 - icz^2}}{z + s - s_0 - i\sigma_0\varepsilon}. \quad (\text{C4})$$

By a linear transformation of the variables

$$u = z + s, \quad v = \frac{cz}{a-c} + \frac{as}{a-c}, \quad (\text{C5})$$

the double integral splits into a product of two single integrals

$$I_1 = -\lim_{\varepsilon \rightarrow 0} \int_{-\infty}^{\infty} dv e^{i(a-c)v^2} \int_{-\infty}^{\infty} du \frac{e^{-i\frac{ac}{a-c}u^2}}{u - s_0 - i\sigma_0\varepsilon}. \quad (\text{C6})$$

In (C6) the integral over  $v$  can be computed easily. Furthermore, the denominator in the  $u$ -integral can be expressed in terms of an integral

$$\begin{aligned}
I_1 &= -i\sigma_0 \sqrt{\frac{\pi}{-i(a-c)}} \lim_{\varepsilon \rightarrow 0} \int_{-\infty}^{\infty} du \int_0^{\infty} dw e^{-i\frac{ac}{a-c}u^2 - i\sigma_0 w(u - s_0 - i\sigma_0\varepsilon)} \\
&= -i\sigma_0 \sqrt{\frac{\pi}{-i(a-c)}} \sqrt{\frac{\pi(a-c)}{iac}} \int_0^{\infty} dw e^{i\frac{a-c}{4ac}w^2 + i|s_0|w} \\
&= -\frac{i\pi\sqrt{\pi}\sigma_0}{\sqrt{-i(a-c)}} \exp\left\{-\frac{iacs_0^2}{a-c}\right\} \operatorname{erfc}\left\{-i|s_0|\sqrt{\frac{iac}{a-c}}\right\}. \tag{C7}
\end{aligned}$$

The whole result  $I = I_0 + I_1$  is given by

$$I = \frac{i\pi\sqrt{\pi}\sigma_0}{\sqrt{-i(a-c)}} \exp\left\{-\frac{iacs_0^2}{a-c}\right\} \left[ \operatorname{erfc}\left\{\frac{-ia|s_0|}{\sqrt{-i(a-c)}}\right\} - \operatorname{erfc}\left\{-i|s_0|\sqrt{\frac{iac}{a-c}}\right\} \right]. \tag{C8}$$

It is convenient to rewrite this result in a form in which the phases of the complex arguments of the error functions are always between  $-\pi/2$  and  $\pi/2$ . This can be done by considering all the possible cases for the signs of  $a$  and  $(a-c)$  separately and using the relation  $\operatorname{erfc}(z) = 2 - \operatorname{erfc}(-z)$ . The results for the different cases can be combined again and written in the form

$$I = \frac{\tau\sigma_0\pi\sqrt{\pi}}{\sqrt{|a-c|}} e^{i\frac{\pi}{4}(1 + \sigma_a + \tau)} \exp\left\{-\frac{iacs_0^2}{a-c}\right\} \left[ \operatorname{erfc}\left\{\frac{|as_0|}{\sqrt{i(a-c)}}\right\} - \operatorname{erfc}\left\{|s_0|\sqrt{\frac{ac}{i(a-c)}}\right\} \right], \tag{C9}$$

where  $\sigma_a = \operatorname{sign}(a)$  and  $\tau = \operatorname{sign}(a/(a-c))$ .

## Appendix D Curved wedges

In this section we discuss the effect of curved wedges on the contributions of diffractive orbits to the level density. The uniform approximation (54) has been derived for a boundary with zero curvature on both sides of the corner. It has to be modified for curved wedges, otherwise the sum of diffractive and periodic orbit contributions is not continuous any more as an optical boundary is crossed. Additional complications can arise due to surface diffraction effects, i. e. creeping orbit or whispering orbit contributions can interfere with the diffractive orbit contributions. We will discuss when these effects have to be taken into account, but we will modify the uniform approximation only in those regions in which these additional effects can be neglected.

The modified formula is derived by using a method of Ref. [16] for obtaining a uniform approximation for the Green function in the case of a curved wedge (see also Ref. [17]). We refer to the original references for a discussion of this method and state here only the result which consists of a change of the argument of the Fresnel function in (21) such that the approximation is continuous across an optical boundary. For the diffractive orbit contribution to the level density, this has the consequence

that only the stability matrix  $M$  is changed in Eqs. (52,53,54): there are additional contributions to  $M$  from reflections on the curved boundary.

In order to discuss these modifications, we first list several properties of geometrical orbits corresponding to an optical boundary which is specified by the values of  $\sigma$ ,  $\eta$  and  $n_{\sigma,\eta}$ . In particular, we consider the trajectories which contribute to the Green function and list for them the number of reflections on the boundary and the side of the corner on which the first reflection occurs. Furthermore, we give restrictions for the numbers  $n_{\sigma,\eta}$  which are implied by their definition.

- $\sigma = +1, \eta = +1$ :  $n_{\sigma,\eta} \geq 0$ ,  $(2n_{\sigma,\eta})$  reflections, first on the line  $\theta = \gamma$ .
- $\sigma = +1, \eta = -1$ :  $n_{\sigma,\eta} \leq 0$ ,  $(-2n_{\sigma,\eta})$  reflections, first on the line  $\theta = 0$ .
- $\sigma = -1, \eta = +1$ :  $n_{\sigma,\eta} \geq 0$ ,  $(2n_{\sigma,\eta} - 1)$  reflections, first on the line  $\theta = \gamma$ . If  $n_{\sigma,\eta} = 0$  the optical boundary cannot be reached. This case can occur only for  $\gamma > \pi$ .
- $\sigma = -1, \eta = -1$ :  $n_{\sigma,\eta} \leq 1$ ,  $(1 - 2n_{\sigma,\eta})$  reflections, first on the line  $\theta = 0$ . The optical boundary cannot be reached if  $n_{\sigma,\eta} = 1$ . This case can occur only for  $\gamma > \pi$ .

With these properties we can now discuss the modification of the stability matrix  $M$  in the case of curved wedges:  $M$  then has an additional contribution for every of the reflections mentioned above. In the following we denote the limits of the radii of curvature as the corner is approached from either side by  $R_0$  and  $R_\gamma$  where the first one corresponds to the side  $\theta = 0$  and the second one to  $\theta = \gamma$ . Then  $M$  has to be replaced by  $BM$  where

$$B = \begin{pmatrix} 1 & 0 \\ -b & 1 \end{pmatrix}. \quad (\text{D1})$$

and

$$b = \begin{cases} \sum_{j=1}^{n_{\sigma,\eta}} \frac{2}{R_0 \sin(2j\gamma - \theta_1)} + \sum_{j=0}^{n_{\sigma,\eta}-1} \frac{2}{R_\gamma \sin((2j+1)\gamma - \theta_1)} & \text{if } \sigma = +1, \eta = +1 \\ \sum_{j=0}^{-n_{\sigma,\eta}-1} \frac{2}{R_0 \sin(2j\gamma + \theta_1)} + \sum_{j=1}^{-n_{\sigma,\eta}} \frac{2}{R_\gamma \sin((2j-1)\gamma + \theta_1)} & \text{if } \sigma = +1, \eta = -1 \\ \sum_{j=1}^{n_{\sigma,\eta}-1} \frac{2}{R_0 \sin(2j\gamma - \theta_1)} + \sum_{j=0}^{n_{\sigma,\eta}-1} \frac{2}{R_\gamma \sin((2j+1)\gamma - \theta_1)} & \text{if } \sigma = -1, \eta = +1 \\ \sum_{j=0}^{-n_{\sigma,\eta}} \frac{2}{R_0 \sin(2j\gamma + \theta_1)} + \sum_{j=1}^{-n_{\sigma,\eta}} \frac{2}{R_\gamma \sin((2j-1)\gamma + \theta_1)} & \text{if } \sigma = -1, \eta = -1 \end{cases} \quad (\text{D2})$$

This approximation is only valid as long as all sine-functions in (D2) are positive and not close to zero. The case of an almost vanishing sine-function corresponds to almost grazing incidence on a side of the corner. Then surface diffraction effects become important and interfere with the diffractive orbit contribution, and the uniform approximation is no longer valid. In the case that some sine-functions are negative and not small, the orbit is not close to an optical boundary and the GTD-approximation can be used (it is the same as in the case of non-curved wedges).

There is a disadvantage of the definition of  $B$  given above. Since there are two possibilities for choosing  $\theta_1$  and  $\theta_2$  corresponding to the two arms of a diffractive orbit in a corner, it follows from (D2) that the uniform approximation is not uniquely defined. (Note that both cases have to be checked for deciding whether surface diffraction effects are important.)

The non-uniqueness of the approximation is a direct consequence of the fact that the uniform approximation for the Green function of Ref. [16] is not symmetric under  $\theta_1 \leftrightarrow \theta_2$ . It is another example for the non-uniqueness of uniform approximations (cf. the discussion in Sec. 2.3). However, as an optical boundary is approached both choices give the same result as they should. Let us discuss in more detail the difference between these two choices. It can be shown that interchanging  $\theta_1$  and  $\theta_2$  amounts to evaluate (D2) with  $\theta_1 = \sigma\theta_2 + 2n_{\sigma,\eta}\gamma - \eta\pi$  instead of  $\theta_1$ . This then directly suggests a possible way by which this ambiguity can be removed, namely by replacing  $\theta_1$  in (D2) by the average of both values which is  $(\theta_1 + \sigma\theta_2 + 2n_{\sigma,\eta}\gamma - \eta\pi)/2$ . As an optical boundary is approached this combination again becomes identical to  $\theta_1$ .

## References

- [1] M. C. Gutzwiller, *Chaos in Classical and Quantum Mechanics* (Springer-Verlag, New-York, 1990).
- [2] R. Balian and C. Bloch, *Ann. Phys. NY* **60**, 401 (1970).
- [3] R. Balian and C. Bloch, *Ann. Phys. NY* **69**, 76 (1972).
- [4] G. Vattay, A. Wirzba and P. E. Rosenqvist, *Phys. Rev. Lett.* **73**, 2304 (1994); G. Vattay, A. Wirzba and P. E. Rosenqvist, *Proceedings of the international conference on Dynamical Systems and Chaos*, Tokyo, edited by Y. Aizawa, S. Saito and K. Shiraiwa (World Scientific, Singapore, 1995), page 463; P. E. Rosenqvist, G. Vattay and A. Wirzba, *J. Stat. Phys.* **83**, 243 (1996).
- [5] N. D. Whelan, *Phys. Rev. E* **51**, 3778 (1995).
- [6] N. Pavloff and C. Schmit, *Phys. Rev. Lett.* **75**, 61 (1995), *erratum* in *Phys. Rev. Lett.* **75**, 3779 (1995).
- [7] H. Primack, H. Schanz, U. Smilansky and I. Ussishkin, *Phys. Rev. Lett.* **76**, 1615 (1996).
- [8] H. Bruus and N. D. Whelan, *Nonlinearity* **9**, 1023 (1996).
- [9] J. B. Keller, *J. Opt. Soc. Amer.* **52**, 116 (1962).
- [10] W. Pauli, *Phys. Rev.* **54**, 924 (1938).
- [11] R. M. Lewis and J. Boersma, *J. Math. Phys.* **10**, 2291 (1969).
- [12] D. S. Ahluwalia, R. M. Lewis and J. Boersma, *SIAM J. Appl. Math.* **16**, 783 (1968).
- [13] D. S. Ahluwalia, *SIAM J. Appl. Math.* **18**, 287 (1970).
- [14] S.-W. Lee and G. A. Deschamps, *IEEE Trans. Antennas & Propag.* **AP-24**, 25 (1976).
- [15] P. C. Clemmow, *Quart. J. Mech. and Appl. Math.* **3**, 241 (1950).



- [16] R. G. Kouyoumjian and P. H. Pathak, Proc. IEEE **62**, 1448 (1974).
- [17] G. L. James, *Geometrical Theory of Diffraction for Electromagnetic Waves* (Peregrinus, Stevenage, 1976).
- [18] J. Boersma, Q. J. Mech. Appl. Math. **28**, 405 (1975).
- [19] S. W. Lee and J. Boersma, J. Math. Phys. **16**, 1746 (1975).
- [20] R. Mittra and Y. Rahmat-Samii in *Electromagnetic Scattering*, edited by P.L.E. Uslenghi (Academic Press, New-York, 1978), page 121.
- [21] M. Schneider and R. J. Luebbers, IEEE Trans. Antennas & Propag. **AP-39**, 8 (1991).
- [22] A. Sommerfeld, *Optics* (Academic Press, New-York, 1954).
- [23] H. S. Carslaw, Proc. London Math. Soc. (Ser. 1) **30**, 121 (1899).
- [24] H. S. Carslaw, Proc. London Math. Soc. (Ser. 2) **18**, 291 (1920).
- [25] *Handbook of Mathematical Functions*, edited by M. Abramowitz and I. A. Stegun (Dover, New-York, 1972).
- [26] M. V. Berry and M. Wilkinson, Proc. R. Soc. Lond. A **392**, 15 (1984).
- [27] E. B. Bogomolny, Nonlinearity **5**, 805 (1992).
- [28] T. Harayama and A. Shudo, Phys. Lett. A **165**, 417 (1992).
- [29] D. Alonso and P. Gaspard, J. Phys. A: Math. Gen. **27**, 1599 (1994).
- [30] B. Burmeister and F. Steiner, “Exact Trace Formula for Quantum Billiards”, Ulm preprint in preparation.
- [31] C. Pisani, “Exploring periodic orbit expansions and renormalisation with the quantum triangular billiard”, preprint 1996, to appear in Ann. Phys.
- [32] C. Schmit, in *Chaos and Quantum Mechanics*, edited by M.-J. Giannoni, A. Voros and J. Zinn-Justin, Les Houches Summer School Lectures LII, 1989 (North-Holland, Amsterdam, 1991), page 331.
- [33] S. C. Creagh, J. M. Robbins and R. G. Littlejohn, Phys. Rev. A **42** 1907 (1990).
- [34] T. Hesse, “Trace Formula for a Non-Convex Billiard System”, Ulm preprint in preparation.